Contents list available at CBIORE journal website

International Journal of Renewable Energy Development

Journal homepage: https://ijred.cbiore.id

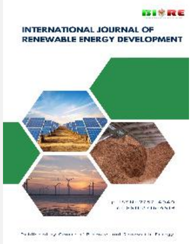

Research Article

Techno-economic assessment and strategic proposal for designing and optimizing the required powered battery for an electric motorcycle under varying driving cycle tests

Tan-Thich Do[a,b], Tan-Ngoc Dinh[c], Vinh-Dat Ly[c*]

[a]*Department of Electrical and Mechatronics, Lac Hong University, Vietnam*

[b]*Department of Mechanical Engineering and Advanced Institute of Manufacturing with High-tech Innovations, National Chung Cheng University, Taiwan*

[c]*Internal Combustion Engine Department, Faculty of Vehicle and Energy Engineering, Ho Chi Minh City University of Technology and Education, Vietnam*

Abstract. Recently, many countries have committed to achieving net-zero emissions by 2050, making the adoption of electric motorcycles increasingly significant. The expansion of electric motorcycles has gained popularity due to their affordability, ease of use, and environmental benefits. In the design of electric motorcycles, optimizing energy efficiency and economic viability both technologically and economically is a key consideration. This study focuses on developing a mathematical model and strategic proposal with the step-by-step calculation for determining the required power battery for electric motorcycles under various driving cycle tests, implemented using Matlab software. The results analyze and discuss the effects of operating conditions on the electric motorcycle's dynamic performance, average energy consumption, and battery cell and pack characteristics. Ultimately, the battery pack optimization strategy was proposed and conducted using the Mixed-Integer Linear Programming (MILP) approach. As a result, the Toshiba battery trademark was identified as the optimal choice for the required power battery in the electric motorcycle, considering both technological effectiveness and economic factors. The Toshiba battery pack has a capacity of 39 Ah, 17 cells, a mass of 13.94 kg, and a cost of $459, respectively. After designing and optimizing the required battery pack for the electric motorcycle, the model was validated to ensure that the pack's energy exceeds the average energy consumption under varying driving cycle tests. Therefore, the model demonstrates high reliability. This study provides valuable insights into designing and evaluating the dynamic performance and battery pack characteristics of electric motorcycles.

Keywords: electric motorcycle's dynamic performance, energy consumption, battery pack optimization strategy, technological effectiveness and economic factors, driving cycle test, Mixed-Integer Linear Programming (MILP).

Received: 10th July 2025; Revised: 17th Sept 2025; Accepted: 29th Sept 2025; Available online: 11th Oct 2025

1. Introduction

Nowadays, climate change, global warming, and air pollution are intensifying worldwide due to traditional emissions, particularly those from fossil fuels (Arshad *et al.* 2024; Li *et al.* 2023; Driga *et al.* 2019). To protect the environment and human health, various solutions have been proposed, including the adoption of renewable energy sources. Recently, the use of green energy in transportation has gained significant popularity. In particular, electric motorcycles are increasingly used in many countries because they are affordable, convenient, and produce zero emissions (Guerra *et al.* 2019; Huang *et al.* 2018; Awirya *et al.* 2023; Murtiningrum *et al.* 2022). However, the electric motorcycle has a challenged duration of the electric motorcycle operation because it depends on the required battery power (Morandin *et al.* 2014). Therefore, the study of the battery's dynamics and power requirements is essential for balancing technological advancement with economic considerations.

To design a battery that meets the power requirements of an electric motorcycle, it is essential to consider the vehicle's dynamic behavior. In this context, (Sharp *et al.* 2004) presented advanced modeling and simulation of electric motorcycle dynamics under various operating conditions. Their results provided valuable insights into electric motorcycle behavior. (Hanifah *et al.* 2019) modeled and simulated motorcycle dynamics to estimate travel range and speed tracking under different driving cycles, demonstrating the model's capability to predict distance and track speed accurately. (Du *et al.* 2009) used Matlab/Simulink to model electric bike dynamics and evaluate ride comfort, revealing that the model suits its original design purpose. Zaripov *et al.* (2019) investigated electric bicycle dynamics under varying conditions, showing that energy efficiency is significantly influenced by dynamic parameters during operation. (Thejasree *et al.* 2019) developed a mathematical model to analyze the longitudinal dynamics of electric motorcycles, offering deeper insights into their behavior. More recently, (Salman *et al.* 2025) developed and validated a dynamic model through experimental testing, showing strong agreement between the model and real-world data. (Qu *et al.* 2017) studied electric bicycle dynamics under external forces and found the model to be highly reliable.

* Corresponding author
Email: datlv@hcmute.edu.vn (V.D.Ly)

(Abagnale *et al.* 2015) created a model to assess both the dynamics and environmental impact of electric bicycles, contributing significantly to performance evaluation and environmental analysis. (Yuniarto *et al.* 2022) conducted modeling, simulation, and validation of electric bicycle energy consumption in an Indonesian case study. They concluded that the model showed high accuracy, with energy consumption errors of −4.7% and −8.63% during real-time driving and dynamometer testing, respectively. (Zhu *et al.* 2008) proposed a mathematical model using multibody dynamics to analyze bicycle motion, achieving good agreement with commercial simulation tools. To further improve modeling accuracy, (Hima *et al.* 2007) developed an 11-degree-of-freedom mathematical model based on the Lagrange formulation, offering a detailed analysis of dynamic behavior under various conditions. (Moreno Giner *et al.* 2009) presented a motorcycle dynamics model focusing on cornering analysis using Maple software, identifying key parameters that influence stability and control. (Arricale *et al.* 2021) developed a nonlinear dynamic model of an electric bicycle using commercial software and introduced a control strategy to regulate motorcycle speed using a Proportional-Integral-Derivative (PID) controller. Their results demonstrated high modeling accuracy. To make the significance of the dynamics performance, several researchers have investigated the dynamics and energy efficiency of hybrid electric motorcycles. (Asaei *et al.* 2010; Asaei *et al.* 2013) designed and implemented hybrid configurations to evaluate performance and fuel consumption, examining two different energy control strategies and demonstrating that hybridization enhances performance while reducing both fuel consumption and emissions. (Chen *et al.* 2004) modeled and controlled a hybrid electric motorcycle equipped with an in-hub wheel motor, reporting an 11.6% improvement in fuel consumption. (Nguyen *et al.* 2017) developed a computational model, revealing that hybrid electric motorcycles can achieve a 21.1% reduction in fuel consumption. Furthermore, (Nguyen *et al.* 2018) analyzed energy consumption and operating costs, highlighting the economic as well as environmental advantages of hybrid electric motorcycles. Recently, (Niccolai *et al.* 2025) proposed and optimized a strategy of the powertrain system to achieve the minimum energy consumption for the electric motorcycle. They revealed that the energy consumption is reduced by up to 22.36% when using their proposal strategy. While (Li *et al.* 2025) studied the fatigue behavior of the motorcycle frame to investigate the dynamics under complex working conditions. They optimized the stiffness of the suspension system and indicated at 15 and 10 N mm^{-1} for the front suspension and rear suspension system, respectively. (Alagmy *et al.* 2024) designed and developed the powertrain system for the electric motorcycle using the SolidWorks and Matlab/Simulink software, considering the cost factor. Their method involved conducting experiments and analyzing the dynamic performances, and indicated cost-effectiveness.

To achieve long-distance operation of an electric motorcycle, the battery-powered system must be carefully considered during vehicle operation. (Chen *et al.* 2021) designed and tested a battery module for electric motorcycles, reporting a low voltage error between measurement and design 1% at 18 A and 0.5% at 9 A. (Fahma *et al.* 2024) developed a battery model that accounted for the financial implications of using high-power batteries in electric motorcycles. (LeBel *et al.* 2018) proposed a model to evaluate battery pack sizing, providing a detailed analysis of how different cell configurations influence overall pack size. (Brodsky *et al.* 2016) designed, optimized, and validated a battery pack for electric motorcycles. Their results confirmed the suitability of the design in terms of meeting power demands and minimizing heat generation. More recently, (Kusumah *et al.* 2025) determined the power requirements of an electric motorcycle using a 72 V, 21 Ah $LiFePO_4$ battery. They concluded that the battery pack could deliver 11.51 HP at a speed of 86 km h^{-1}. (Esparza *et al.* 2020) developed a battery pack for an electric motorcycle prototype and validated it under various conditions, confirming its capability to supply sufficient propulsion power. To analyze the thermal behavior of the battery, (Shahjalal *et al.* 2022) developed a numerical battery model and concluded that a cooling system is essential to maintain optimal temperature during high-acceleration scenarios. (Arifwardana *et al.* 2022) compared the thermal performance of NMC and $LiFePO_4$ batteries during operation and found that NMC cells exhibited higher temperatures. (Elbeshbeshy *et al.* 2023) used Matlab/Simulink to design a 48 V, 350 Wh battery pack, which was experimentally validated and found suitable for electric motorcycle propulsion. (Nugraha *et al.* 2022) analyzed power demands under various charge capacities, identifying a 48 V, 15 Ah Li-ion battery as appropriate. (Aprillia *et al.* 2023) designed and tested a 72 V, 40 Ah battery pack on a dynamometer, noting that it reached full charge at 71 V. (Nguyen *et al.* 2020) designed and optimized the battery pack characteristics and operating cost for a hybrid electric motorcycle converted from a Honda Lead 110 cc. They concluded that a 48 V – 33 Ah battery pack is suitable for the model, and that adopting the hybrid configuration results in cost savings. During the design of the electric motorcycle, the required battery pack system energy plays a crucial role in supplying the electricity for the auxiliary loads of the electric motorcycle, while the required battery pack energy depends on the energy consumption. (Niccolai *et al.* 2024) analyzed the energy consumption of the electric motorcycle, considering the recovery energy from the regenerative braking system. Their results discussed the potential of regenerative energy for the energy consumption in the system. (Syahrobi *et al.* 2025) analyzed the characteristics of the Li-ion battery in the electric motorcycle. They tested it under various roads, such as uphill, flat road, and speed variations of 50, 30, and 10 km h^{-1}. Their results indicated that the battery temperature increased when the electric motorcycle operated at high velocity, but the voltage during the charging and discharging process is stable, thus the Lion battery is suitable for the application of the electric motorcycle. (Izzaturrahman *et al.* 2025) designed the required powered battery pack with the specifications of Li-ion 1865 cells battery type and capacity of 24 Ah, and voltage of 64 V for an electric motorcycle. They revealed that the capacity and voltage were achieved at 23.36 Ah and 69.67 V, respectively, during the battery pack charging process. Additionally, the battery pack can provide power for the electric motor up to 1.54 HP and a maximum velocity of 34 km h^{-1} in the dynamometer test.

Based on the reviewed literature, electric motorcycles play a crucial role in achieving net-zero emissions by 2050 in many countries. Their growing popularity is attributed to ease of use, convenience, and affordability. Therefore, enhancing electric motorcycle performance and understanding the dynamic behavior, required battery power, and energy consumption are essential. In this study, a mathematical model was developed to simulate the dynamic performance and battery characteristics of an electric motorcycle under various driving cycle tests. The model was implemented using Matlab/Simulink with a step-by-step calculation approach. The basic blocks included Constant, Function, From, To, Display, and Mathematical. Subsystems were created to simplify the model and facilitate management. Data recording was performed using the Workspace platform in the software. The effects of different operating conditions on the motorcycle's dynamic performance and energy consumption were analyzed. Furthermore, the required battery power and characteristics were evaluated for different battery types.

Table 1
The NYCC characteristics of the driving cycle test

Description	Value
Total duration / s	598
Total distance / m	1898
Maximum speed / km h^{-1}	44.6
Average speed / km h^{-1}	11.4
Percentage of time stopped (%)	23
Number of stops	16
Maximum acceleration / m s^{-2}	2.68
Maximum deceleration / m s^{-2}	−3.13
Idle time / s	140
Acceleration phases	19
Deceleration phases	18

Table 2
The WLTP Class 1 characteristics of the driving cycle test

Description	Low	Medium	Total
Duration / s	589	433	1022
Distance / m	3324	4767	8091
Stop time / s	155	48	203
% of stop	26.3%	11.1%	37.4%
Highest acceleration / m s^{-2}	0.76	0.63	–
Minimum acceleration / m s^{-2}	−1.00	−0.57	–
Mean velocity without stops / km h^{-1}	27.6	44.6	36.1
Highest velocity / km h^{-1}	49.1	64.4	–
Mean velocity with stops / km h^{-1}	20.3	39.6	29.85

Finally, a strategy was proposed to optimize the power requirements of the electric motorcycle. This study is significant for guiding the design of battery systems in electric motorcycles. Additionally, the developed model can predict dynamic performance, estimate energy consumption, and determine cell and pack-level battery characteristics across diverse driving conditions.

2. Description of the mathematical model

To facilitate and simplify the modeling and evaluation of the electric motorcycle dynamics, determination of the required powered battery, and optimization of the battery pack under driving cycle test in this study, several assumptions are made as follows:

a. The traction force of the electric motorcycle is considered with a longitudinal electric motorcycle, ignoring side forces effect with the horizontal and vertical planes of the electric motorcycle.
b. The tire-road adhesion and aerodynamic drag coefficient are constant values.
c. The tire of an electric motorcycle is rolling without slipping on the road.
d. The battery pack operates at near-optimal temperature; aging or degradation, capacity fade, and thermal derating are neglected.
e. Battery pack layout (series/parallel) is electrically uniform; interconnect resistance and cell dispersion are neglected.

2.1 Driving cycle test description

To evaluate the dynamic performance of the electric motorcycle, a driving cycle test was employed in this study. In this section, the characteristics of three driving cycle tests are described in detail in this section.

The New York City Cycle (NYCC) driving cycle test was conducted in New York City, reflecting typical stop-and-go traffic conditions. The characteristics of the NYCC driving cycle test are summarized in Table 1, and the distance, velocity, and acceleration profiles are shown in Fig. S1 (in the Supplementary material).

The Worldwide Harmonized Light Vehicle Test Procedure (WLTP) is classified into three categories: WLTP Class 1, Class 2, and Class 3. The power-to-mass ratio (PMR), measured in W kg^{-1}, is used to determine which WLTP class the dynamic system belongs to. The PMR is defined as follows:

$$PMR = \frac{P_{EM}}{M_{EM}} \tag{1}$$

Where: P_{EM} and M_{EM} represent the rated power output of the electric motorcycle (W) and the mass of the electric motorcycle (kg) without load person, respectively. Additionally, WLTP Class 1 is selected when the $PMR \leq 22$, WLTP Class 2 is chosen

Table 3
The FTP-75 characteristics of the driving cycle test

Description	Value
Duration / s	2474
Distance / m	17769
% of stop	17.9
Highest acceleration / m s^{-2}	1.47
Minimum acceleration / m s^{-2}	−1.47
Mean velocity without stops / km h^{-1}	41.6
Highest velocity / km h^{-1}	91.2
Mean velocity with stops / km h^{-1}	34.1

when $22 < PMR \leq 34$, and WLTP Class 3 is selected when $PMR > 34$.

In this study, the rated power of the electric motorcycle is 1800 W, and its mass is 130 kg. Therefore, the PMR is calculated to be 15.84 W kg^{-1}, which is less than 22 W kg^{-1}. As a result, WLTP Class 1 is suitable for modeling and simulating the electric motorcycle. The driving cycle test is typically used for vehicles with low power and velocities under 70 km h^{-1}. The driving cycle test includes velocity stages of low-medium-low. Additionally, the characteristics of WLTP Class 1 are summarized in Table 2, and the distance, velocity, and acceleration profiles are shown in Fig. S2 (in the Supplementary material).

The Federal Test Procedure 75 (FTP-75) driving cycle test was employed in this study. This driving cycle test, which was developed by the United States Environmental Protection Agency (US-EPA), was conducted in urban conditions (Makarchuk *et al.* 2015). The key characteristics of the FTP-75 driving cycle are summarized in Table 3, and the distance, velocity, and acceleration profiles are illustrated in Fig. S3 (in the Supplementary material).

2.2 Electric motorcycle dynamic performance model

During the operation of an electric motorcycle, various forces act upon it, including aerodynamic resistance force, acceleration force, climbing resistance force, and rolling resistance force, as described in Fig. 1. The electric motorcycle's stability and longitudinal forward dynamic were assumed in this study. According to Newton's Second Law, the relationship between these resistance forces and the traction force is described as follows:

$$F_T = F_{Ad} + F_A + F_C + F_R \qquad (2)$$

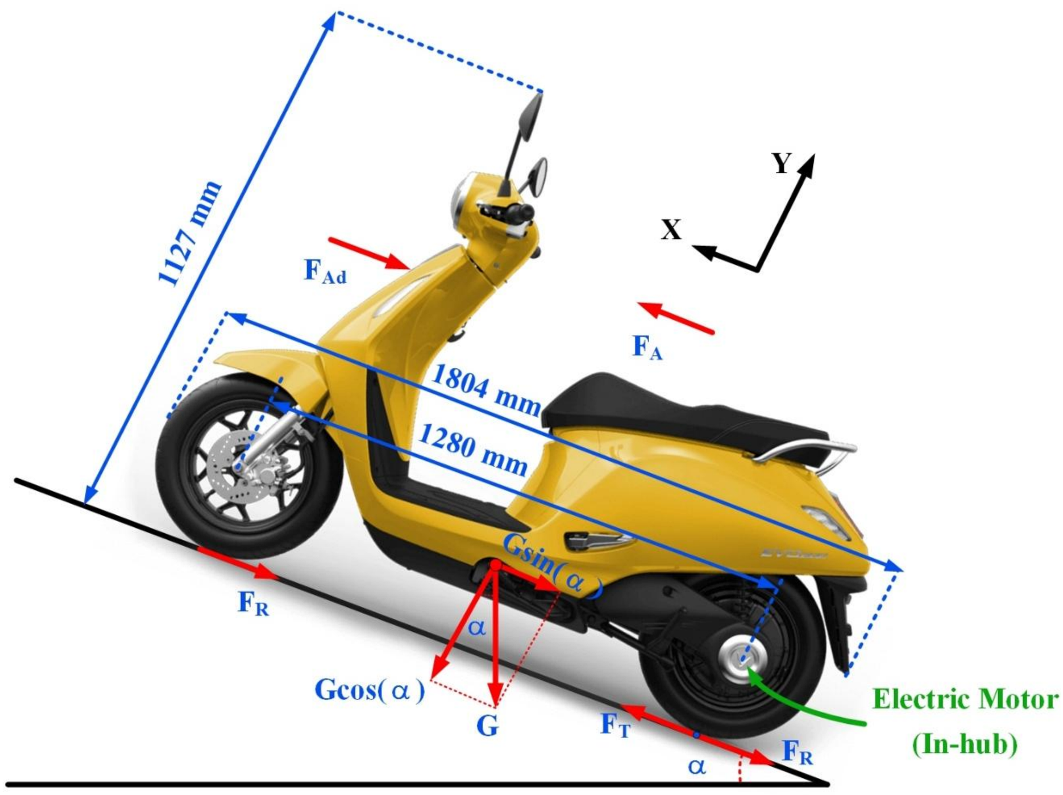

Fig. 1 Electric motorcycle dynamic performance and basic dimensions

Where: F_T, F_{Ad}, F_A, F_C, F_R represent the traction force, aerodynamic resistance force, acceleration force, climbing resistance force, and rolling resistance force. All forces are units in N.

The aerodynamic resistance force is proportional to the square of the electric motorcycle's speed and is calculated using Eq. (3):

$$F_{Ad} = \frac{1}{2} A_f C_d \rho_{air} V^2 \tag{3}$$

Where: A_f is the front area of the electric motorcycle, in m^2; C_d denotes the aerodynamic drag coefficient ($C_d = 0.2 - 1.0$); ρ_{air} represents the air density ($\rho_{air} = 1.25\ kg\ m^{-3}$); and V is the speed of the electric motorcycle, in m s^{-1}.

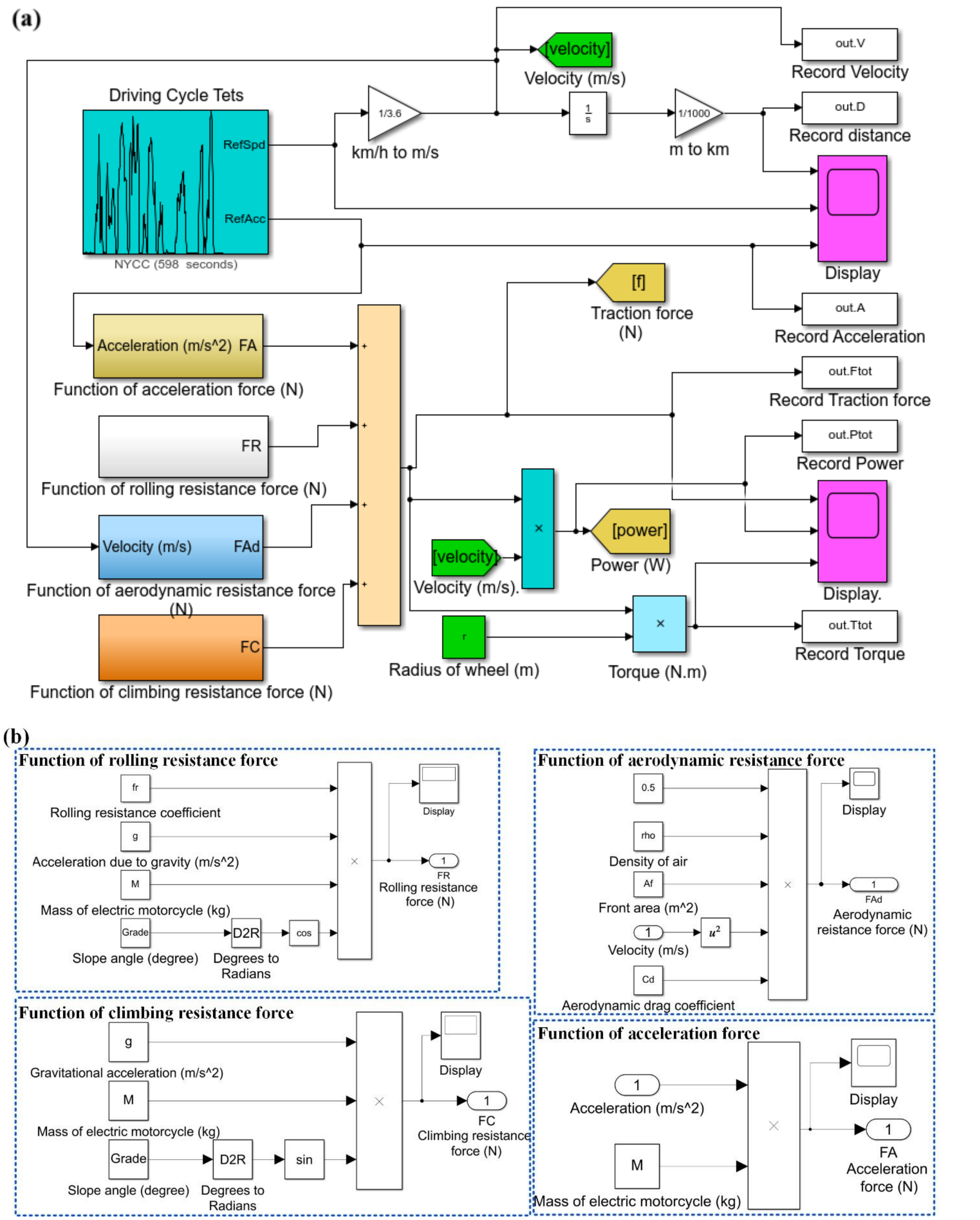

Fig. 2 The electric motorcycle's dynamic performance under the driving cycle test (a); The detailed function of the forces in the electric motorcycle (b)

The acceleration force represents the electric motorcycle's ability to accelerate and depends on its mass and velocity. It is defined by Eq. (4):

$$F_A = M_{EM}\frac{dV}{dt} \quad (4)$$

Where: M_{EM}, and V denote the electric motorcycle mass in kg; and the velocity of the electric motorcycle, in km h^{-1}, respectively.

When the electric motorcycle operates on a hill, a climbing resistance force is generated. Conversely, when the motorcycle moves on a flat road, this resistance force is negligible. The climbing resistance force is determined using the following equation:

$$F_C = gM_{EM}sin(\alpha) \quad (5)$$

Where: g, M_{EM}, and α represent the gravitational acceleration ($g = 9.81\ m\ s^{-2}$); the mass of the electric motorcycle, in kg; and the slope angle (degree), respectively.

The rolling resistance force opposes the motion of the wheel and is determined using Eq. (6):

$$F_R = M_{EM}gC_R cos(\alpha) \quad (6)$$

Where: C_R is the rolling coefficient. It depends on the quality of the road.

In this study, the transmission system is an in-hub type, meaning the power from the electric motor is transferred directly to the wheel. Consequently, the power and torque of the electric motorcycle are defined by Eq. (7) and Eq. (8), respectively:

$$P_{EM} = F_T V \quad (7)$$

$$T_{EM} = F_T R_w \quad (8)$$

Where: R_w is the radius of the wheel of the electric motorcycle, in m.

From Eqs. (2) to (8), the dynamic performance of the electric motorcycle was modeled and is illustrated in Fig. 2 (a). Additionally, the detailed representation of the resistance forces in the electric motorcycle is shown in Fig. 2 (b).

The input parameters of the electric motorcycle are listed in Table 4. Indeed, the Evo200 Vinfast, which was manufactured in Vietnam, was selected for modeling and simulation in this study (VinFast, 2025).

2.3 Modeling the average energy consumption for the propulsion system and auxiliary loads

In this study, the average energy of the propulsion system, in Wh km^{-1}, was calculated based on the driving cycle test:

$$E_{ap} = \frac{E_S}{d} \quad (9)$$

Where: E_S is the total energy consumption in the driving cycle test, in Wh; and d denotes the length of the driving cycle test, in km, respectively.

Additionally, the total energy consumption was estimated based on the driving cycle test. It was shown in Eq. (10):

$$E_s = \int P_{EM}dt \quad (10)$$

During the electric motorcycle operation in the driving cycle test, auxiliary loads (Wh km^{-1}) were consumed, including both permanent and intermittent loads. Notably, intermittent loads account for 10% of the total auxiliary consumption. Therefore, the average energy consumption of the auxiliary loads should be considered and is determined using Eq. (11). Additionally, the auxiliary power consumption of the electric motorcycle is presented in Table 5 (VinFast. *n.d.*).

$$E_{aux} = \frac{P_{aux}\Delta t}{d} \quad (11)$$

Where: P_{aux}, and Δt denote the auxiliary consumption power, in W; and the duration of the driving cycle test, in s.

Ultimately, the total average energy consumption, in Wh km^{-1}, comprises the average energy consumption of the propulsion system and the average energy consumption of the auxiliary loads. It is defined by Eq. (12):

Table 4
The specific parameters and input parameters of the electric motorcycle of Evo200 Vinfast

Parameter	Value	Unit
Aerodynamic drag coefficient	0.6	–
Gravitational acceleration	9.81	m s^{-2}
Rolling resistance coefficient	0.011	–
Front area of an electric motorcycle	0.6	m^2
Transmission efficiency	90	%
Trunk volume	20	L
Dimension (Length x Width x Height)	1804 x 683 x 1127	mm
Wheelbase	1280	mm
Electric motorcycle mass	130	kg
Ground clearance	150	mm
Electric motor type	In-hub	–

Table 5
The auxiliary power in the Evo200 Vinfast

Auxiliary power type	Description	Value (W)	Total (W)
Permanent auxiliary loads	Headlight (high beam) system	35	59
	Battery management system	18	
	Screen information light system	6.0	
Interrupt auxiliary loads (account for 10%)	Horn system	15	3.48
	Signal light system	10.24	
	Braking light system	9.6	

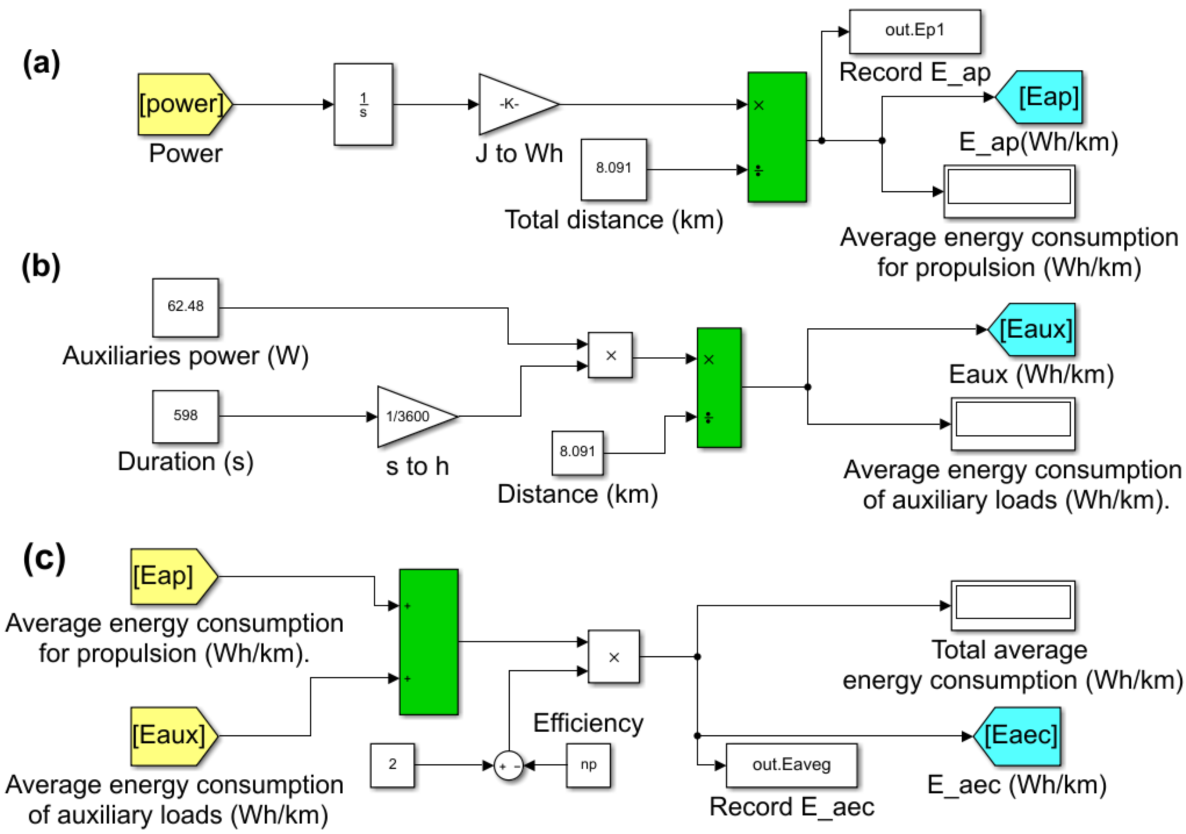

Fig. 3 Modeling the average energy consumption: (a) for the propulsion system, (b) auxiliary loads, and (c) total average energy consumption

$$E_{aec} = \left(E_{aux} + E_{ap}\right) * \left(2 - \eta_p\right) \tag{12}$$

Where: η_p is the efficiency of the transmission.

From Eqs. (9) to (12), the electric motorcycle dynamic performance model was modeled and described in Fig. 3.

2.4 Mathematical model of the battery power characteristics

2.4.1 Modeling the basic parameters of the cell battery

In this section, the dimensional parameters and characteristics of the battery were analyzed in detail under different battery configurations. Nowadays, the configuration of the pouch and cylindrical batteries are widely used in vehicles. To achieve high voltage, a large number of battery cells are connected in series. Additionally, multiple series-connected battery packs are arranged in parallel to increase capacity. The assembled battery pack is then enclosed in a protective casing. The battery connection structure is illustrated in Fig. 4.

The cell battery energy (E_{cb}), in Wh, can be determined based on the cell voltage and cell battery capacity. It was defined by Eq. (13):

$$E_{cb} = U_{cb} C_{cb} \tag{13}$$

Where: U_{cb} and C_{cb} corresponding to the cell voltage of the battery (in V) and cell capacity (in Ah).

Additionally, the volume energy density (E_v), in Wh m^{-3}, or weight energy density (E_g), in Wh kg^{-3}, was calculated by the cell battery energy by its volume or mass, respectively. These are defined in Eq. (14) and Eq. (15):

$$E_v = \frac{E_{cb}}{V_{cv(c),(p)}} \tag{14}$$

$$E_g = \frac{E_{cb}}{m_{cb}} \tag{15}$$

Where: $V_{cv(c),(p)}$ represents the volume of the cell battery for the cylindrical configuration or pouch configuration, in m^{-3}; and m_{cb} denotes the mass of the cell battery, in kg.

Since the dimensional parameters of the cell battery different between cylindrical and pouch configurations, the determination of cell volume also varies. The volume of the cell battery for the cylindrical and pouch configurations is determined using Eq. (16) and Eq. (17), respectively.

$$V_{cv(c)} = \frac{\pi D_c^2}{4} H_c \tag{16}$$

$$V_{cv(p)} = T_p W_p H_p \tag{17}$$

Where: D_c represents the diameter of the cell battery for a cylindrical configuration; H_c is the height of the cell battery for the cylindrical configuration. For the pouch configuration, T_p, W_p, and H_p denotes the thickness, width, and height of the cell battery, respectively, as shown in Fig. 4 (b). All the dimension parameters are in units of m.

From Eq. (13) to (17), the cell battery characteristics were modeled and shown in Fig. S4 (in the Supplementary material). It consists of the basic dimensions, volume, and mass of the cell battery.

During the design of the battery pack energy (E_{bp}), in Wh, the average energy consumption in the driving cycle test must be carefully considered to ensure sufficient energy supply for

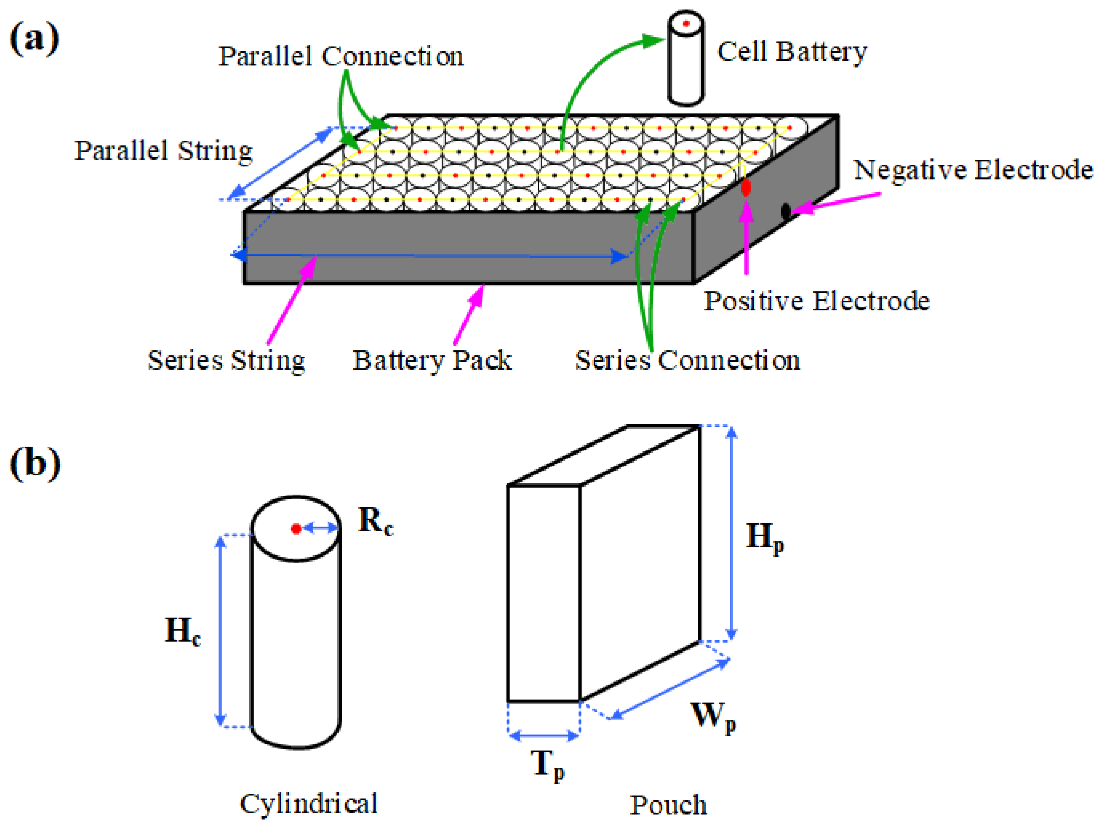

Fig. 4 (a) Arrangement of the cell battery; (b) Dimension parameters of the cell battery

both the propulsion system and auxiliary loads of the electric motorcycle. To ensure sufficient energy for the electric motorcycle to complete the travel distance, the requirement is established by the following conditions:

$$E_{bp} \geq E_{aec} \times d \tag{18}$$

The minimum required battery pack energy must balance the average energy consumption and is dependent on the length of the driving cycle test, as expressed in Eq. (19):

$$E_{bp} = E_{aec} \times d \tag{19}$$

When cell batteries are connected in series, they form a series battery string, which determines the battery pack voltage (U_{bp}). The total voltage of the series battery string is the sum of the individual cell voltages (U_{cb}). Therefore, the number of cells in the series battery string is estimated using Eq. (20) and must be an integer value:

$$N_{cs} = \frac{U_{bp}}{U_{cb}} \tag{20}$$

The series battery string energy (E_{bs}) is determined by multiplying the number of cells in the series battery string by the energy of an individual cell:

$$E_{bs} = N_{cs}E_{cb} \tag{21}$$

To increase the capacity of the battery pack, a series of battery strings are connected in parallel. The number of parallel-connected series battery strings is determined and must be an integer, as shown in Eq. (22):

$$M_{sp} = \frac{E_{bp}}{E_{bs}} \tag{22}$$

The battery pack capacity, in Ah, is calculated by multiplying the number of parallel-connected series battery strings by the capacity of an individual cell. This is defined by Eq. (23) as follows:

$$C_{bp} = M_{sp}C_{cb} \tag{23}$$

Additionally, the total number of cells in the battery pack (N_{cp}) can be estimated by multiplying the number of cells in the series battery string by the number of parallel-connected series battery strings, as described by Eq. (24):

$$N_{cp} = N_{cs}M_{sp} \tag{24}$$

Eq. (25) and Eq. (26) are used to determine the battery pack volume (V_{bp}), in m^{-3}, and the mass of the battery pack (m_{bp}), in kg. These are calculated as follows:

$$V_{bp} = N_{cp}V_{cv(c),(p)} \tag{25}$$

$$m_{bp} = N_{cp}m_{cb} \tag{26}$$

From Eq. (18) to Eq. (26), the battery pack was modeled and described in Fig. S5 (in the Supplementary material).

2.4.2 Modeling the designed battery pack with the high-voltage system

Fig. S6 (in the Supplementary material) shows the modeling of the designed battery pack with a high-voltage system in this section. The maximum current in series battery string (I_{mcss}), in A, is calculated based on the maximum the ratio of the charge-

Table 6
Specification of the cell battery with the cylindrical and pouch configuration under the FTP-75

Manufacturer	Group 1			Group 2		
	LG Chem (DNK Power, 2022)	**Samsung** (DNK Power, 2019)	**DNK** (DNK Power, 2025)	**Evlithum** (EVLithium, 2025)	**A123** (Buy A123 Products, 2025)	**Toshiba** (EVLithium. 2025)
Model	INR21700M50LT	INR21700 50E	DNK 21700	SLPB 7570270	AMP20 M1HD	A123 39AH NCM
Geometry type	Cylindrical	Cylindrical	Cylindrical	Pouch	Pouch	Pouch
$Cost_{cb}$	5.0	3.33	3.0	72	30	27
C_{cb}	5.76	4.9	5.0	32	19.5	39
U_{cb}	3.69	3.6	3.6	3.65	3.3	3.65
C_{max}	3.0	1.0	2.0	7.0	10	13.65
C_{rate}	0.2	0.5	0.2	1.0	1.0	1.5
M_{cb}	0.0682	0.069	0.071	0.395	0.496	0.820
W_{cb}	0	0	0	8.8	16.0	22.8
T_{cb}	0	0	0	1.08	0.725	0.702
H_{cb}	7.06	7.08	7.09	18.80	22.70	26.80
D_{cb}	2.144	2.025	2.110	0	0	0
Cycle life	1000	500	500	500	3000	3000
Chemistry	Li-ion	Li-ion	LiNCA	$LiNi_xCo_yMn_zO_2$	LiFePO4	$LiFePO_4$
T_C	0 to 45	0 to 45	0 to 45	−20 to 55	−30 to 55	0 to 45
T_D	−20 to 55	−20 to 60	−20 to 60	−20 to 55	−40 to 60	−20 to 50

discharge (C_{rate_max}), in h⁻¹, and cell battery capacity (C_{cb}), in Ah, as described in Eq. (27):

$$I_{mcss} = C_{rate\_max} C_{cb} \quad (27)$$

The maximum current in the battery pack (I_{mcbp}), in A, depends on the maximum current in the series battery string (I_{mcss}), in A, and the number of parallel-connected series battery strings (M_{sp}). The relationship is defined by Eq. (28):

$$I_{mcbp} = M_{sp} I_{mcss} \quad (28)$$

The maximum power of the battery pack (P_{mbp}), in W, is calculated based on the maximum current in the battery pack (I_{mcbp}), in A, and battery pack voltage (U_{bp}), in V, using the following formula:

$$P_{mbp} = U_{bp} I_{mcbp} \quad (29)$$

The continuous current in a string (I_{ccs}), in A, is estimated using the equation Eq. (30). It depends on the cell battery capacity (C_{cb}), in Ah, and the ratio of charge-discharge (C_{rate}), in h^{-1}, as follows:

$$I_{ccs} = C_{cb} C_{rate} \quad (30)$$

The battery pack's continuous current (I_{bpcc}), in A, and the battery pack's continuous power (P_{bpcp}), in W, are determined corresponding to Eq. (31) and Eq. (32), as follows:

$$I_{bpcc} = I_{ccs} M_{sp} \quad (31)$$

$$P_{bpcp} = U_{bp} I_{bpcc} \quad (32)$$

In addition, the cost of the battery pack was calculated to evaluate the effectiveness of economics by varying the batteries in this study. The cost of the battery pack, in $, was determined based on the manufacturer and shown as follows:

$$Cost_{bp} = N_{cs} M_{sp} Cost_{cb} \quad (33)$$

Where: $Cost_{cb}$ is the cost of a cell battery, in $.

From the datasheet of the manufacturer, the specifications of the cell battery and the cost of the cell battery with the configuration of cylindrical and pouch are listed in Table 6. Group 1 included the cell battery with the cylindrical configuration, and Group 2 consisted of the cell battery with the pouch configuration.

2.5 Proposal strategy to optimize the battery pack

In this study, the calculation and design of the required powered battery for an electric motorcycle were thoroughly analyzed in the previous section. However, economic and technological effectiveness considering factors such as cost, performance, and the weight or volume of the battery pack, was also critically evaluated. In other words, the two key factors of energy and economy (2EE) were emphasized in this section. Mixed-Integer Linear Programming (MILP) is a mathematical optimization technique that can be used to optimize various parameters in battery pack design. In this context, MILP helps minimize costs, maximize performance, and enforce constraints such as weight and volume. The optimization process was conducted in a Matlab software environment. The following equations define the constraint conditions for this proposed strategy: the general objective function is presented in Eq. (34), while the constraint conditions are described in Eqs. (35) to (39):

$$f(x) = min \sum_i A_i x_i \; with \; x_i \in \{0,1\} \, \forall i \quad (34)$$

Where: A_i represents the input parameters of the i-th battery pack, which are related to the economy and technology parameters, x_i is the binary decision variable of the ith battery pack.

For technological effectiveness, the total required power battery pack must meet or exceed the estimated energy consumption, which was derived from the driving cycle test. This relationship is expressed in Eq. (35). Additionally, the capacity of the battery pack should be higher than 30 Ah (Zahedi *et al.* 2024), as depicted in Eq. (36):

$$\sum_i E_{bp_i} x_i \geq E_{aec} \quad (35)$$

$$\sum_i C_{bp_i} x_i \geq C_{min} \quad (36)$$

Where: C_{min} is the minimum capacity of the battery pack, in Ah.

For the dimensional factor, the total volume and mass of the battery pack should not exceed the available space and predefined limits. The volume and mass constraints are described in Eq. (37) and Eq. (38), respectively:

$$\sum_i V_{bp_i} x_i \leq V_{max} \quad (37)$$

$$\sum_i m_{bp_i} x_i \leq m_{max} \quad (38)$$

Where: V_{max} and m_{max} denote the expected maximum volume limit, in L, and the expected maximum volume limit, in kg, respectively.

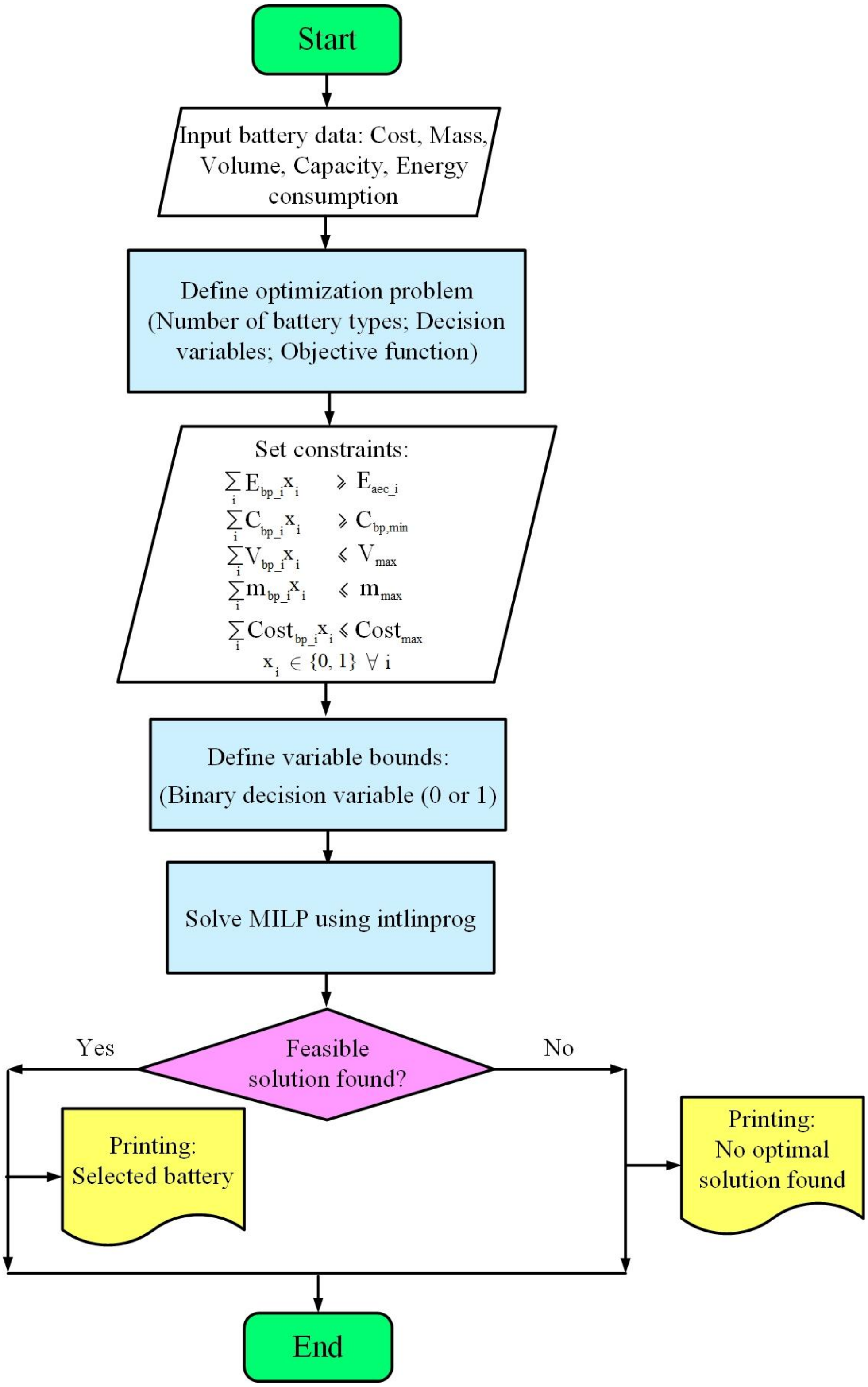

Fig. 5 The flowchart of the proposal strategy to optimize the battery pack for an electric motorcycle, using MILP

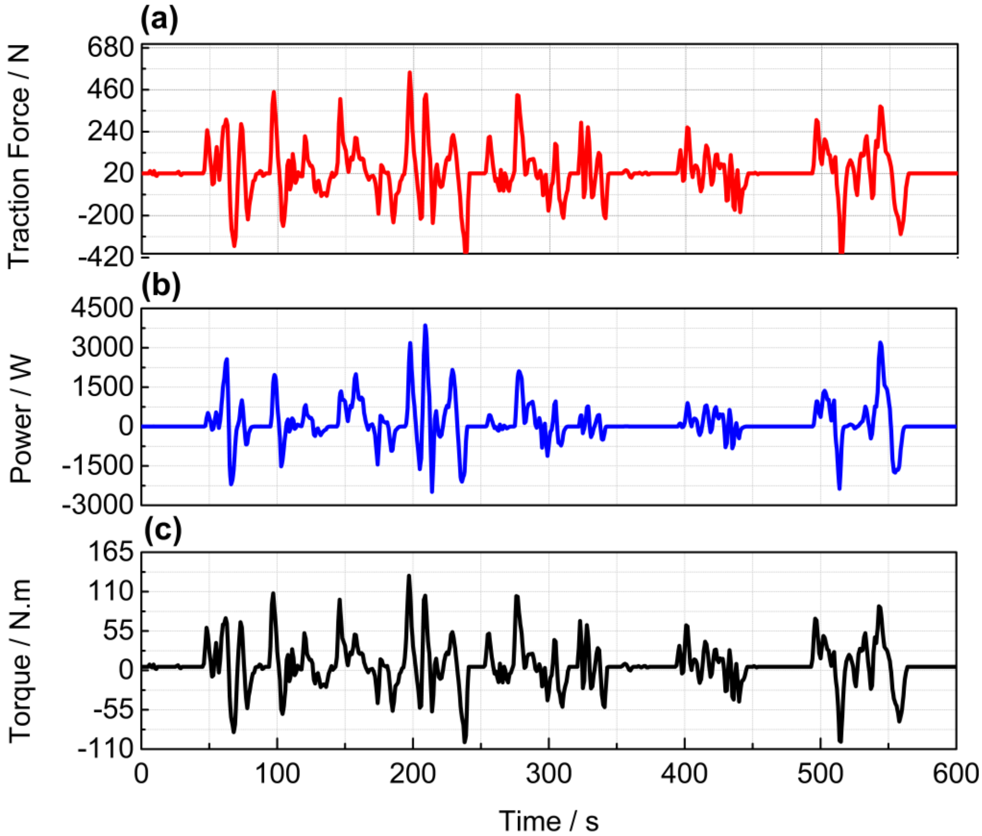

Fig. 6 Electric motorcycle dynamic performance under NYCC driving cycle test: (a) Traction force; (b) Power; and (c) Torque

For economic effectiveness, the cost of the battery pack should be minimized while remaining feasible for purchasing the electric motorcycle. The cost constraint is established in Eq. (39):

$$\sum_i Cost_{bp_i} x_i \le Cost_{min} \tag{39}$$

Where: $Cost_{bp_i}$ represents the total cost of battery pack in the ith battery pack, in \$. $Cost_{min}$ denotes the expected minimum cost limit, in \$.

From Eqs. (35) to (39), the relationship between technological effectiveness, dimensional constraints, and economic constraints is expressed as a system of equations, as follows:

$$\begin{cases} \sum_i E_{bp_i} x_i \ge E_{aec\_i} \\ \sum_i C_{bp_i} x_i \ge C_{min} \\ \sum_i V_{bp_i} x_i \le V_{max} \\ \sum_i m_{bp_i} x_i \le m_{max} \\ \sum_i Cost_{bp_i} x_i \le Cost_{min} \\ x_i \in \{0,1\}\ \forall i \end{cases} \tag{40}$$

In this study, the MILP approach was used to determine the optimal battery pack and implemented in the Matlab software environment using the "intlinprog" function solver, owing to its capability of efficiently solving minimization problems in MILP problems, which enables efficient and accurate solutions (Willis *et al.* 2017; MathWorks, 2024). The flowchart of the MILP solver process in this study is shown in Fig. 5.

2.6 Validation of battery pack energy at the best choice of the trademark battery

To evaluate the required battery pack energy and ensure that the required battery pack energy is greater than the energy consumption in this study, which is to ensure sufficient energy for the vehicle to complete the travel distance. The model should be validated in this context. In fact, the battery pack energy, average energy consumption, and remaining battery pack energy can be described using the energy balance law, as follows:

$$\textit{Remaining energy} = \textit{Energy of pack} - \textit{Energy consumed} \tag{41}$$

$$E_{rebp} = \frac{E_{bp}}{d} - E_{aec} \tag{42}$$

Where: E_{rebp} is the remaining battery pack energy, in Wh km $^{-1}$; E_{bp} represents the battery pack energy, in Wh; d is the distance of the driving cycle test, in km; and E_{aec} denotes the average energy consumption, in Wh km $^{-1}$.

The state of charge (SOC) represents the percentage of the remaining battery pack energy during electric motorcycle operation under a driving cycle. The SOC can be calculated using Eq. (43) (Wenzl, 2009):

$$SOC(t) = SOC(t_0) - \frac{1}{3600}\int_0^t \frac{I(t)\eta_{batt}}{C_{bp}}\,dt \tag{43}$$

Where: $SOC(t_0)$ represents the fully charged battery pack with a value of 1; $I(t)$ denotes the current of discharging, in A; η_{batt} is the coulombic efficiency; t represents the duration of time, in s; and C_{bp} is the battery pack capacity, in Ah.

Therefore, the remaining battery pack energy is calculated based on the SOC, battery pack capacity, and cell battery voltage, as expressed in the following equation:

$$E_{rebp} = \frac{SOC(t)C_{bp}U_{cb}}{d \times Ncp} \tag{44}$$

3. Results and Discussion

3.1 Analysis of the electric motorcycle dynamic performance under varying driving cycle tests

During electric motorcycle operation, various resistance forces influence its performance. Therefore, a detailed analysis of the electric motorcycle's dynamic performance under different driving cycle tests is essential. Fig. 6 illustrates the electric motorcycle's dynamic performance, including traction force, power, and torque under the NYCC driving cycle test. Additionally, Figs S7 and S8 depict the dynamic performance of the electric motorcycle under the WLTP Class 1 and FTP-75 driving cycles, respectively (in the Supplementary material).

Fig. 6 shows the variation in traction force, power, and torque of the electric motorcycle during the NYCC driving cycle test. It can be observed that these parameters change in response to velocity variations throughout the test. At 198th seconds, the traction force and torque reach their maximum values of 550.69 N and 110 N.m, respectively. Additionally, the maximum power was achieved at 3853.91 W at 210th seconds. Determining the maximum power and torque is crucial for selecting a suitable electric motor for the motorcycle. In other words, if the selected motor is inadequate, such as having insufficient power compared to the motorcycle's requirements, it may fail to generate enough traction force to sustain the motorcycle's motion effectively.

Similarly, the electric motorcycle's dynamic performance varied according to the WLTP Class 1 driving cycle test, as shown in Fig. S7 (in the Supplementary material). At the initial stage of the WLTP Class 1 driving cycle test, the traction force and torque reached high values of 170.25 N and 40.86 N.m at the 13th second. This can be attributed to the acceleration of the electric motorcycle at the start of the test. Additionally, the traction force in this driving cycle is lower than in the NYCC driving cycle test, reaching a maximum of 188.08 N when the motorcycle operates at high velocity phase. This occurs because the acceleration in the WLTP Class 1 cycle is lower than in the NYCC driving cycle test. The electric motorcycle's dynamic performance reaches its peak at the high-speed phase, between the 589th and 1022nd seconds.

For the FTP-75 driving cycle test, the variation in the electric motorcycle's dynamic performance is shown in Fig. S8 (in the Supplementary material). It can be observed that the traction force, power, and torque fluctuate frequently throughout the driving cycle due to changes in the motorcycle's acceleration. The highest values recorded for traction force, power, and torque are 354.02 N, and 84.97 N.m, respectively, at 195th

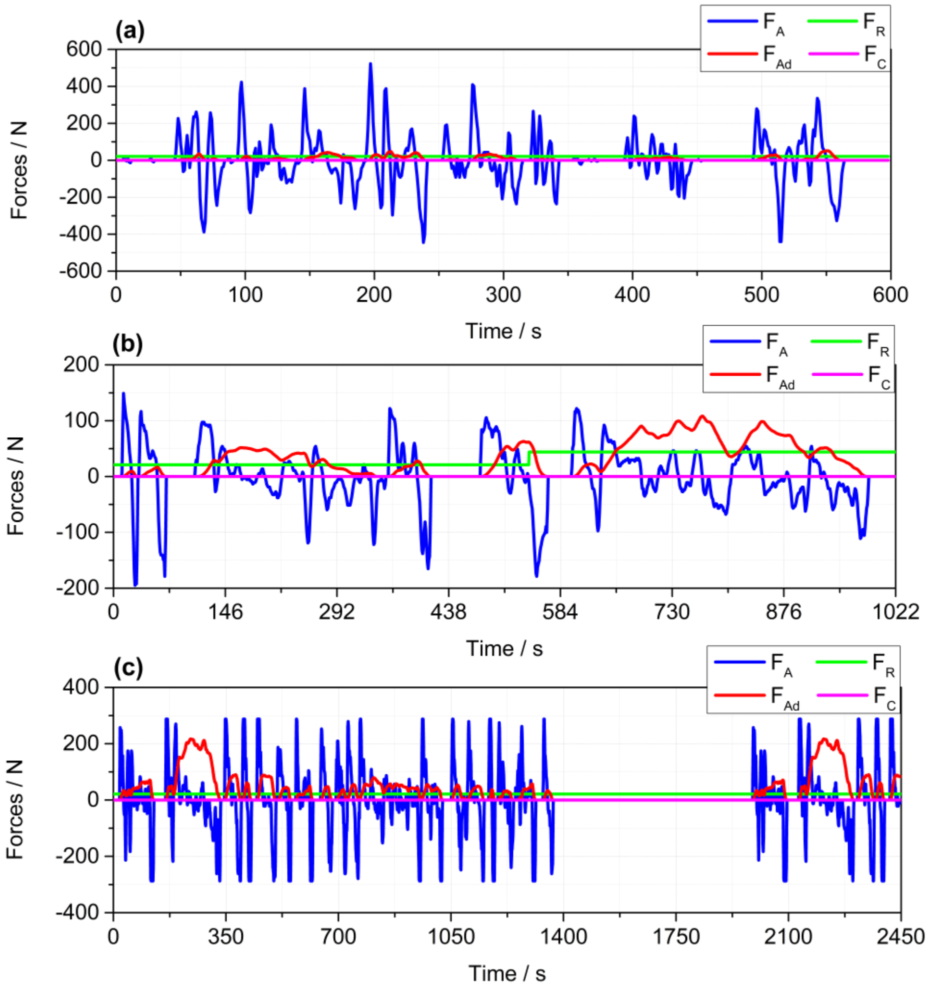

Fig. 7 The variation of the forces during the electric motorcycle operation under varying driving cycle tests: (a) NYCC; (b) WLTP Class 1; and (c) FTP-75

seconds. The maximum power reached 7009.89 W at 226th seconds. From the 1368th seconds to the 1990th seconds, the dynamic performance drops to zero due to the time-off stage of the driving cycle test.

The variation in forces acting on the electric motorcycle is shown in Fig. 7. These forces include the acceleration force, rolling resistance force, aerodynamic drag resistance force, and climbing resistance force under different driving cycles. It can be observed that the acceleration force is the dominant force compared to the rolling resistance, aerodynamic drag resistance, and climbing resistance forces, as it primarily drives the motorcycle forward. The aerodynamic drag resistance force fluctuates depending largely on the motorcycle's velocity. Meanwhile, the climbing resistance force remains zero since the motorcycle operates in a city environment with no slope angles. The rolling resistance force remains constant at 21.04 N because the electric motorcycle operates on a well-maintained road, as shown in Fig. 7 (a) and (c), corresponding to the NYCC and FTP-75 driving cycle tests. However, when the electric motorcycle operates on urban roads between the 589th and 1022nd seconds in the WLTP Class 1, the road quality decreases. Consequently, the rolling resistance force increases to 44.0 N, as depicted in Fig. 7 (b).

3.2 Effect of operating conditions on the electric motorcycle dynamic performance

During electric motorcycle operation, its performance is influenced by various operating conditions. In this section, the effects of motorcycle mass and aerodynamic area are analyzed to evaluate dynamic performance under driving cycle tests. To ensure significance, the NYCC driving cycle test was chosen to assess the impact of motorcycle mass on dynamic performance. Additionally, the WLTP Class 1 driving cycle test was selected to evaluate the effect of aerodynamic area on the motorcycle's dynamic performance.

Fig. 8 illustrates the effect of electric motorcycle mass on dynamic performance under the NYCC driving cycle test, including traction force, acceleration force, power, and torque. It can be observed that as the motorcycle mass increases, the traction force, acceleration force, and rolling resistance force also increase. Specifically, the rolling resistance force reached 14.03 N, 21.04 N, and 28.06 N when the motorcycle mass increased by 130 kg, 195 kg, and 260 kg, respectively, as shown in Fig. 8 (a). Similarly, the power and torque of the electric motorcycle increased with higher mass, as depicted in Figs. 8 (b) and 8 (c). In other words, increasing dynamic power is

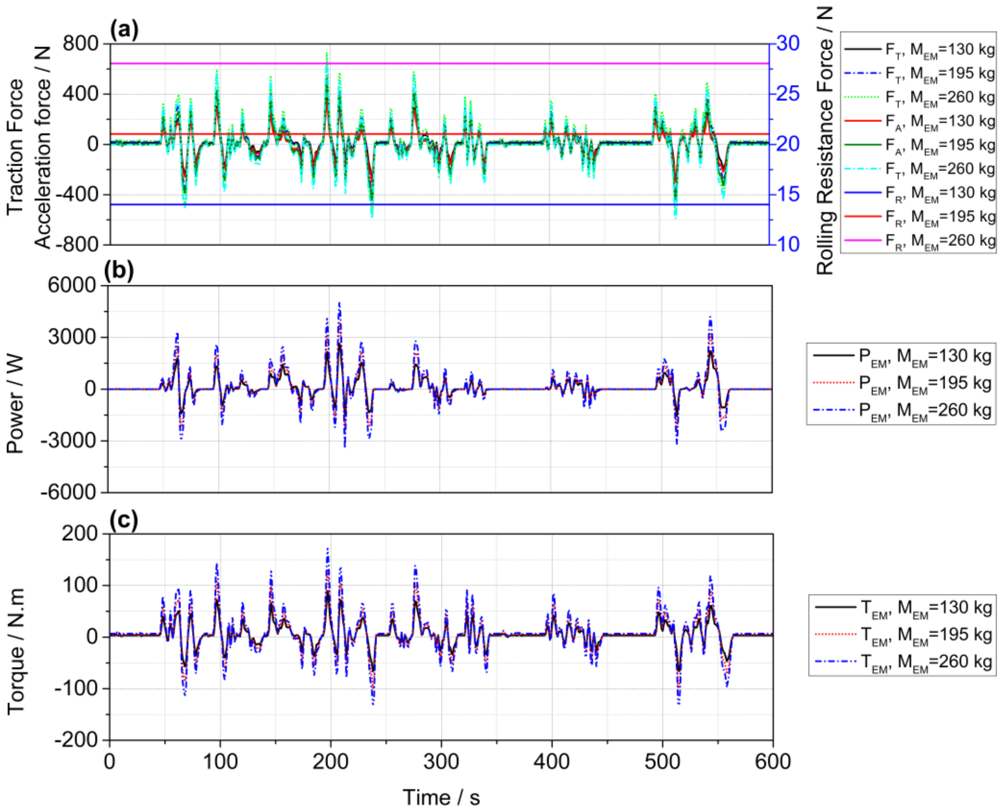

Fig. 8 Effect of electric motorcycle mass on dynamic performance under the NYCC driving cycle test

Table 7
The rolling resistance coefficient under different types of roads

No.	Type of road	C_R (%)	This study
1	Pressed dirty (during rain)	5.0 – 15	0.100
2	Pressed dirty (with dry)	2.5 – 3.5	0.030
3	Snow	3.0 – 5.0	0.045
4	Gravel	2.0 – 2.5	0.025
5	Iced	1.5 – 3.0	0.020
6	Good asphalt or concrete	1.0 – 1.8	0.011
7	Wet sand	6.0 – 15	0.090
8	Pebble with having potholes	3.5 – 5.0	0.045
9	Muddy dirty	10 – 25	0.170

necessary to overcome resistance forces, thereby enhancing performance and enabling the motorcycle to move forward efficiently.

The effect of aerodynamic area on dynamic performance under the WLTP Class 1 test is demonstrated in Fig. 9. It can be observed that as the aerodynamic area increases, both the

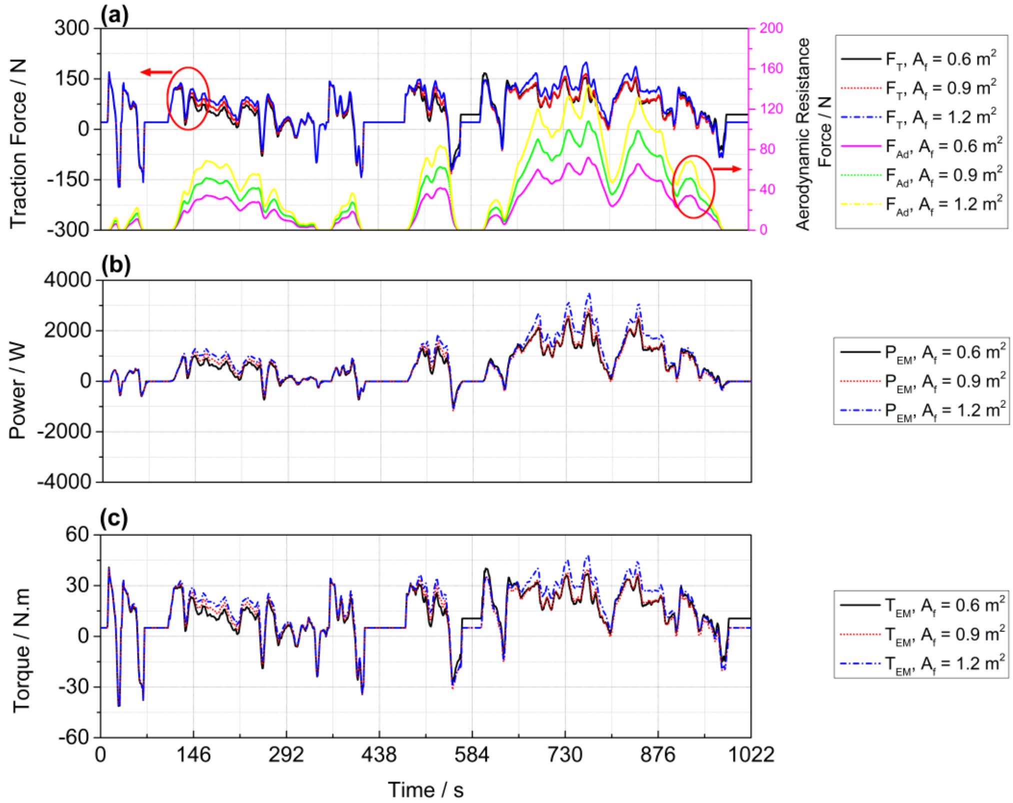

Fig. 9 Effect of aerodynamic area on dynamic performance under WLTP Class 1

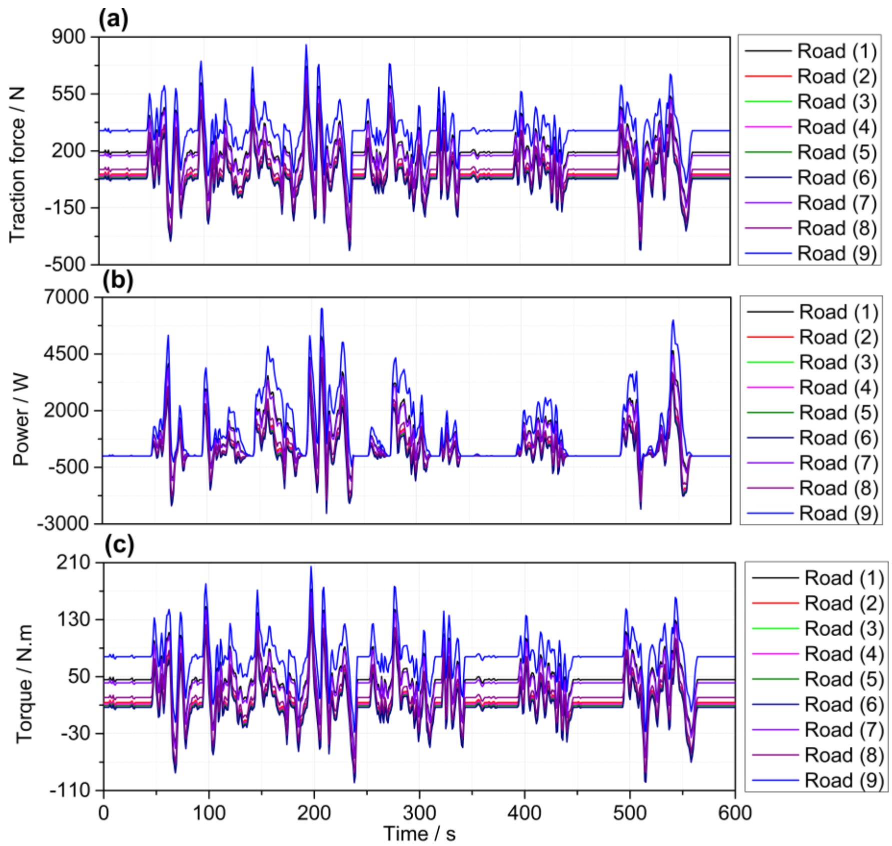

Fig. 10 Effect of road quality on dynamic performance under the NYCC driving cycle

traction force and aerodynamic resistance force also increase. Notably, the aerodynamic resistance force shows a significant difference between 600th seconds and 1000th seconds when the aerodynamic area increases from 0.6 m² to 1.2 m² in increments of 0.3 m², achieving a maximum value of 144 N. This phenomenon can be explained by the fact that the electric motorcycle operates in the high-speed phase during this period. As stated in Eq. (3), the aerodynamic resistance force is proportional to the square of the motorcycle's speed, leading to a more pronounced effect at higher speeds.

To emphasize the importance of surface road quality, which are represented the rolling resistance coefficient, this study analyzed the effect of the rolling resistance coefficient under various road conditions. The rolling resistance coefficients for different road types are listed in Table 7 (Chen *et al.*, 2016). Fig. 10 illustrates the dynamics of the electric motorcycle in the NYCC driving cycle across nine road conditions: good asphalt or concrete, snow, wet dirt (during rain), dry dirt, gravel, wet sand, pebbles with potholes, muddy dirt, and ice. The results show that vehicle dynamics vary significantly depending on the rolling resistance coefficient and the driving cycle. When the motorcycle operates on poor road surfaces, the required traction force, power, and torque increase substantially to adapt to the worst-case scenario. Conversely, under good road conditions, the rolling resistance coefficient is low, resulting in a lower power demand. In this context, the best performance occurs on good asphalt or concrete, while the most demanding case is observed on muddy dirt roads.

3.3 Analysis of the average energy consumption under various driving cycle tests

Fig. 11 shows the average energy consumption of the electric motorcycle, including the average energy consumption of the propulsion system and auxiliary loads, under varying driving cycles of the NYCC, WLTP Class 1, and FTP-75. It can be seen that the average energy consumption gradually increased during the electric motorcycle duration operation in the driving cycle test. Especially, the average energy consumption of the auxiliary is constant at 5.47, 2.19, and 2.41 Wh km^{-1}. Because the average energy consumption was calculated under the length of the driving cycle, leading to the average energy consumption of the NYCC is higher than WLTP Class 1. WLTP Class 1 is superior to the FTP-75.

The determination of the average energy consumption of the electric motorcycle under the driving cycle test aims to establish the conditions for designing the required battery pack. Obviously, the design of the battery pack energy is higher than the average energy consumption of the propulsion system and auxiliary loads. In other words, to sufficient energy supply for the propulsion system and auxiliary load, the average energy of the battery pack should be higher than the average energy consumption.

3.4 Discussion on the required powered battery under the driving cycle test

The characteristics of the cell battery and battery pack under different configurations, including cylindrical and pouch designs, are listed in detail in Table 8. It can be observed that the volume of both the cell battery and battery pack in Group 2 is larger than in Group 1. Consequently, the dimensions of the battery pack box in Group 2 are greater than those in Group 1, though the difference is not significant.

Additionally, the maximum current in a series battery string, the maximum current in the battery pack, the continuous current in a string, the battery pack's continuous current, and the battery pack's continuous power are all higher in Group 2 compared to Group 1. As a result, the required power for the battery pack in Group 2 is greater than that of Group 1. This explains why the cost of the battery pack for Group 2 is higher than that of Group 1.

From the electric motorcycle dynamic performance analysis, the maximum power required was 3853.91 W, 3289.69 W, and 7009.89 W for operation under the NYCC, WLTP Class 1, and FTP-75 driving cycles, respectively. This indicates that the maximum power of the battery pack in Group 1 is insufficient to supply the necessary energy for both the propulsion system and auxiliary loads. In contrast, the

Table 8
Determination of the cell battery and battery pack characteristics

Manufacturer	Group 1			Group 2		
	LG Chem	**Samsung**	**DNK**	**Evlithum**	**A123**	**Toshiba**
Model	INR21700M50LT	INR21700 50E	DNK 21700	SLPB 7570270	AMP20 M1HD	A123 39AH NCM
Geometry type	Cylindrical	Cylindrical	Cylindrical	Pouch	Pouch	Pouch
E_{aec}	18.620	18.620	18.620	18.620	18.620	18.620
$V_{cv(c),(p)}$ x 10^6 L	0.025	0.023	0.025	0.179	0.263	0.429
E_{cb}	21.254	17.640	18.0	116.80	64.350	142.350
E_g	311.648	255.652	253.521	295.696	129.738	173.598
E_v	833.882	773.616	726.058	653.700	244.379	331.857
N_{cs}	17	17	17	17	19	17
E_{bs}	361.325	299.880	306.000	1985.600	1222.650	2419.950
M_{sp}	1.0	1.0	1.0	1.0	1.0	1.0
C_{bp}	5.760	4.90	5.0	32.0	19.50	39.0
N_{cp}	17	17	17	17	19	17
V_{bp}	0.433	0.388	0.421	3.037	5.003	7.292
m_{bp}	1.159	1.173	1.207	6.715	9.424	13.940
I_{mcss}	17.280	4.90	10.0	224.0	195.0	532.350
I_{mcbp}	17.280	4.90	10.0	224.0	195.0	532.350
P_{mbp}	1083.974	299.88	612.0	13899.2	12226.5	33032.318
I_{ccs}	1.152	2.45	1.000	32.0	19.50	58.50
I_{bpcc}	1.152	2.45	1.000	32.0	19.50	58.50
P_{bpcp}	72.265	149.940	61.200	1985.60	1222.65	3629.925
$Cost_{bp}$	85.0	56.61	51.0	1224	570	459

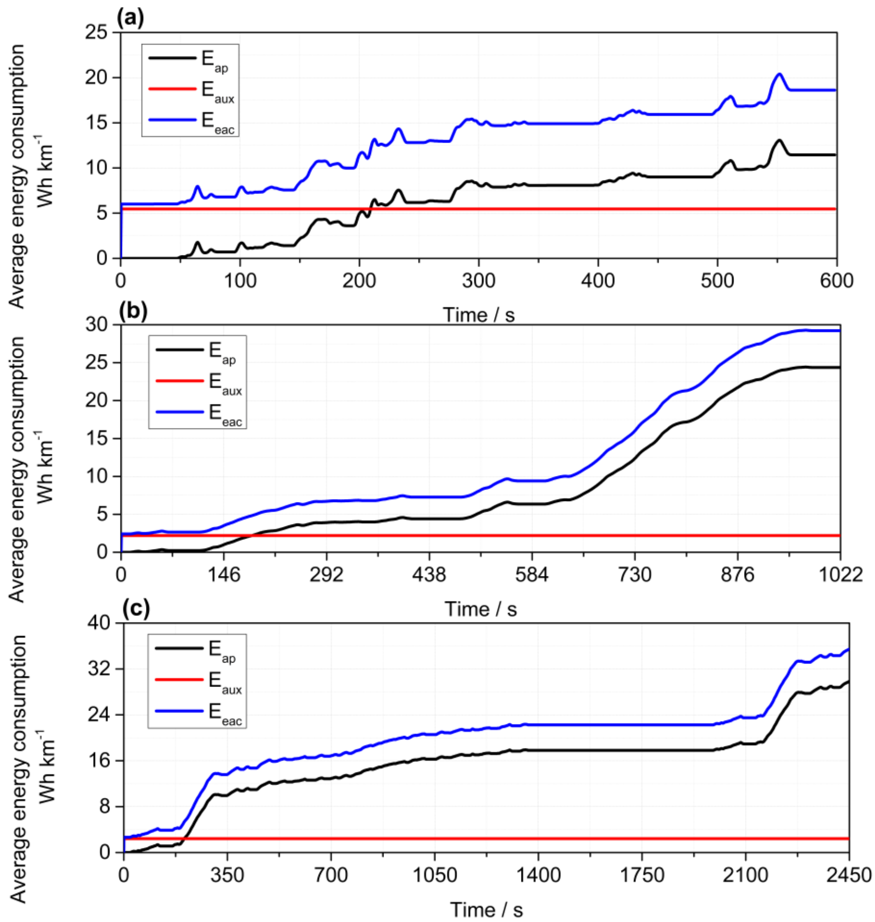

Fig. 11 The variation of the average energy consumption during the electric motorcycle operation under varying driving cycle tests: (a) NYCC; (b) WLTP Class 1; and (c) FTP-75

maximum power of the battery pack in Group 2 exceeds the required power for the electric motorcycle by approximately 3.61, 3.72, and 4.71 times for the Evlithium, A123, and Toshiba battery trademarks, respectively. Therefore, Group 2 is the more suitable choice for designing the required battery pack. However, the best battery pack option will be revealed and analyzed in the next section.

3.5. Analysis of the proposal strategy to optimize the battery pack and validation of the model.

As a result, priority was given to batteries in Group 2, as their maximum power exceeds the electric motorcycle's dynamic performance requirements. In other words, the selected battery pack is capable of supplying sufficient electrical power for both the propulsion system and auxiliary loads during operation. Moreover, both technological effectiveness and economic feasibility must be considered. Based on the proposed MILP-based optimization strategy, the battery pack with the Toshiba trademark emerges as the best choice. This is because it balances both technological performance and cost-effectiveness, making it an affordable and practical option. In this study, the detailed parameter settings, convergence criteria for this solver configuration, and the brief justification for the choice of constraints are listed in Table 9, which is presented in detail in Section 2.5.

After optimizing the battery pack for the electric motorcycle under various driving cycle tests, the proposed strategy identified the Toshiba battery pack as the best choice, balancing both technological and economic factors through the MILP approach. The validation of the battery pack energy under driving cycle tests is therefore essential to support and clarify this study. The validation of battery pack energy at the best choice of the trademark battery is carried out based on equations (41) to (44), which are described in detail in Section 2.6. In addition, according to the design constraints in Eq. (18), the battery pack energy over the driving cycle distance must exceed the average energy consumption, and this was validated against the minimum required pack energy. Furthermore, the safety coefficient in Eq. (12) was considered to ensure that the designed pack could reliably supply energy to the electric motorcycle under worst-case conditions. Therefore, the model is designed and considered under worst-case conditions. This aims to make sure that the electric motorcycle can operate in all realistic conditions.

Fig. 12 illustrates the average energy consumption, total battery pack energy, and remaining battery pack energy during electric motorcycle operation across different driving cycles. The results show that average energy consumption gradually increased, while the battery pack energy also increased and consistently remained above the consumption level to meet demand all the driving cycle test. Meanwhile, the remaining battery pack energy decreased due to auxiliary load power losses. A slight discrepancy between battery pack energy and average energy consumption was observed in the NYCC and WLTP Class 1 cycles, as shown in Fig. 12 (a) and (b). In contrast,

Table 9
Hyperparameter setting of the MILP in this study

Parameter	Description	Value	Unit
Function	"Intlprog" function was used to solve the problem. The solve the minimization problem in this study.	Intlprog	–
Maxtime	This is the runtime limit for solving the problem in this study.	60	s
TolGapRel	TolGapRel stands for Relative Optimality Tolerance (Relative MIP Gap). It defines the stopping criterion based on how close the current solution is to the theoretical optimum (convergence criteria).	10^{-6}	–
Heuristics	It is algorithms that quickly find good feasible solutions to guide the solver and speed up the search.	round	–
CutGeneration	This process adds linear constraints, or cuts, to eliminate infeasible regions without removing feasible integer solutions, tightening the relaxation and accelerating convergence to the optimal solution.	intermediate	–
E_{aec_i}	During the design of the required powered battery for an electric motorcycle, the average energy consumption of the electric motorcycle is considered to ensure sufficient energy for the vehicle to complete the travel distance.	18.62	Wh
C_{min}	The parameter is the minimum capacity of the battery pack in an electric motorcycle. The minimum capacity constraint ensures that the selected battery cells can provide enough energy storage for the electric motorcycle to operate over its required driving range.	30	Ah
V_{max}	This is the maximum battery pack volume in an electric motorcycle because electric motorcycles have very limited space for battery placement, ensuring the selected cells are compact enough to physically fit.	10	L
m_{max}	The parameter is the maximum mass of the battery pack. Limits total battery mass so the pack doesn't make the motorcycle too heavy.	15	kg
$Cost_{min}$	The cost of the battery pack should be as low as possible while remaining affordable, taking economic factors into consideration.	500	$

during the FTP-75 cycle, the two values were much closer due to the longer cycle distance and higher maximum power requirement, which were used to determine the battery pack specifications in the worst case. Overall, the model demonstrates high accuracy and reliability.

4. Conclusions

During the design and calculation of the required power battery pack for the electric motorcycle under varying driving cycle tests, the optimization of both technological and economic effectiveness was considered. Several significant conclusions

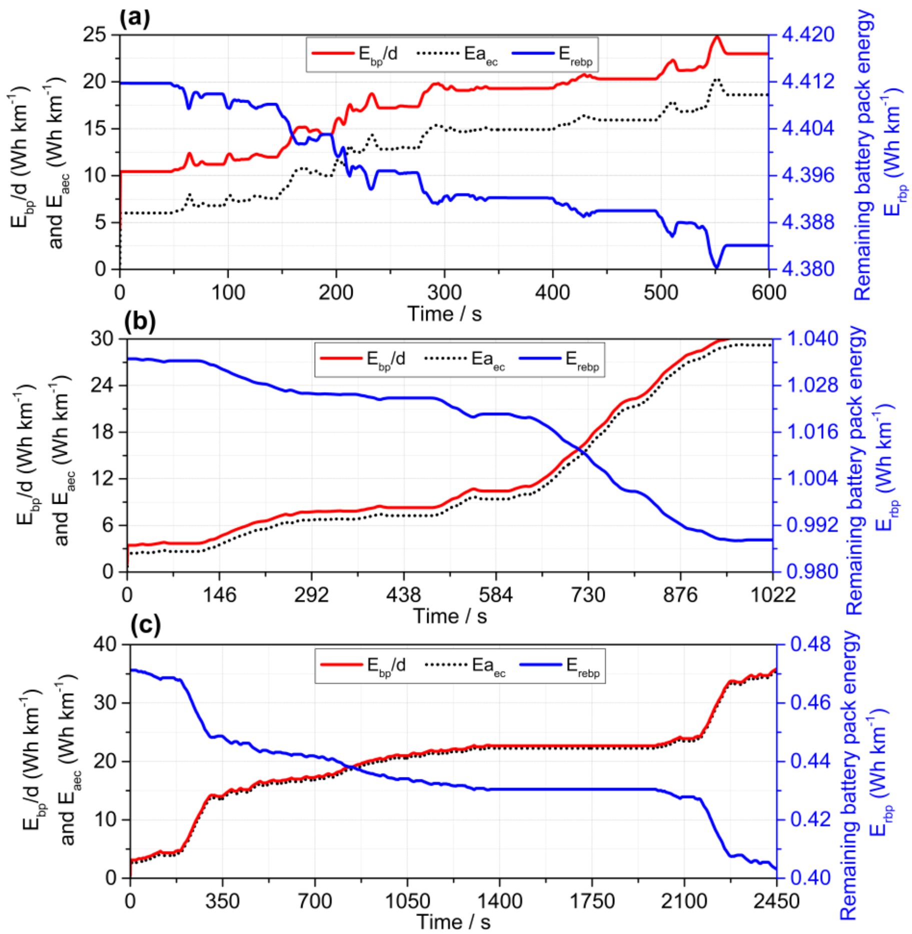

Fig. 12 Validation of battery pack energy under driving cycle test (a) NYCC; (b) WLTP Class 1; and FPT-75

were drawn in this study. Indeed, the effect of operating conditions on the electric motorcycle's dynamic performance was analyzed under various driving cycle tests, including NYCC, WLTP Class 1, and FTP-75. Additionally, estimation of the average energy consumption from various driving cycle tests to aid in the design of the required power battery pack. Furthermore, development of a mathematical model to analyze the characteristics of individual battery cells and the overall battery pack. The proposed strategy for optimizing technological and economic effectiveness in this study utilizes the MILP approach, considering the total required power battery pack, volume, mass, and cost. As a result, the Toshiba battery trademark was identified as the optimal choice for the electric motorcycle's battery pack. After designing and optimizing the required powered battery pack for the electric motorcycle, the model is validated and ensure that the battery pack energy exceeds the average energy consumption under varying driving cycle tests. Therefore, the model achieves high reliability. In addition, the model can be applied to other electric motorcycles and battery types, provided their specifications are available.

Though the electric motorcycle dynamics, required battery pack, and proposal strategy to optimize the battery pack considering the technology and economic factors under varying driving cycle tests were performed in this study. However, several future works are provided. Indeed, the control strategy is being considered to optimize the propulsion system of the electric motorcycle. Design and validate control algorithms (e.g., model predictive control, optimal torque/speed scheduling) to improve energy efficiency and transient performance across driving cycles. Furthermore, the optimization of the battery pack operation and management needs to be conducted by an intelligent control algorithm. Implement AI-based or optimization-based battery management system (BMS) strategies (reinforcement learning, model predictive control, genetic algorithms) to optimize charge/discharge scheduling, extend usable energy, and reduce degradation while respecting safety limits.

Abbreviations and nomenclatures

AI	Artificial Intelligence
A_i	Input parameters of the i-th battery pack
A_f	Front area of the electric motorcycle (m^2)
BMS	Battery management system
$Cost_{cb}$	Cost of the cell battery ($)
C_d	Aerodynamic drag coefficient ($C_d = 0.2 - 1.0$)
C_{cb}	Capacity of the cell battery (Ah)
C_R	Rolling coefficient
C_{max}	Maximum capacity of the cell battery (Ah)
C_{rate_max}	Maximum the ratio of the charge-discharge (h^{-1})
C_{rate}	Ratio of charge-discharge (h^{-1})
$Cost_{bp_i}$	Total cost of battery pack in the ith battery pack ($)
$Cost_{min}$	Expected minimum cost limit ($)
C_{min}	Minimum capacity of the battery pack (Ah)
$Cost_{bp}$	Cost of the battery pack ($)
C_{rate}	Charge-discharge ratio of a cell battery
d	Length of the driving cycle test (km)
D_{cb}	Diameter of the cell battery (cm)
E_{cb}	Cell battery energy (Wh)
E_{bp}	Battery pack energy (Wh)
E_v	Volume energy density (Wh m^{-3})
E_g	Weight energy density (Wh kg^{-3})
E_{ap}	Average energy of the propulsion system (Wh km^{-1})
E_S	Total energy consumption in the driving cycle test (Wh)
E_{aec}	Average energy consumption of the auxiliary loads (Wh km^{-1})
E_{rebp}	Remaining battery pack energy (Wh km $^{-1}$)
E_{aux}	Auxiliary power consumption (Wh km^{-1})
E_{bs}	Series battery string energy (Wh)
FTP-75	Federal Test Procedure 75
F_T	Traction force (N)
F_{Ad}	Aerodynamic resistance force (N)
F_A	Acceleration force (N)
F_C	Climbing resistance force (N)
F_R	Rolling resistance force (N)
g	Gravitational acceleration ($g = 9.81\ m\ s^{-2}$);
H_{cb}	Height of the cell battery (cm)
I_{mcbp}	Maximum current in the battery pack (A)
I_{mcss}	Maximum current in series battery string (A)
I_{bpcc}	Battery pack's continuous current (A)
I_{ccs}	Continuous current in a string (A)
m_{max}	Expected maximum volume limit (kg)
m_{cb}	Mass of the cell battery (kg)
m_{bp}	Mass of the battery pack (kg)
M_{cb}	Weight of cell battery (kg)
M_{sp}	Number of parallel-connected series battery strings
M_{EM}	Electric motorcycle mass (kg)
MILP	Mixed-Integer Linear Programming
N_{cp}	Total number of cells in the battery pack
N_{cs}	Number of cells in the series battery string
NYCC	New York City Cycle
SOC	State of charge
P_{EM}	Power of an electric motorcycle (W)
PMR	The power-to-mass ratio
PID	Proportional-Integral-Derivative
P_{mbp}	Maximum power of the battery pack (W)
P_{bpcp}	Battery pack's continuous power (W)
P_{aux}	Auxiliary consumption power (W)
R_w	Radius of the wheel (m)
T_{cb}	Thickness of the cell battery (cm)
T_C	Operating temperature at charging (°C)
T_D	Operating temperature at discharging (°C)
t	Duration of the time (s)
W_{cb}	Width of the cell battery (cm)
U_{cb}	Potential of the cell battery (V)
U_{bp}	Battery pack voltage (V)
x_i	Binary decision variable of the ith battery pack
V	Speed of the electric motorcycle (m s^{-1})
V_{bp}	Battery pack volume (m^3)
$V_{cv(c),(p)}$	Volume of the cell battery for the cylindrical configuration or pouch configuration (m^3)
V_{max}	Expected maximum volume limit (L)
WLTP	Worldwide Harmonized Light Vehicle Test Procedure
ρ_{air}	Air density ($\rho_{air} = 1.25\ kg\ m^{-3}$)
Δt	Duration of the driving cycle test (s)
η_p	Efficiency of the transmission
η_{batt}	Coulombic efficiency
2EE	Energy and economy

Acknowledgments

This study was conducted with financial support from CCU, LHU, and HCMUTE. The author would like to express sincere gratitude for this support.

Author Contributions: T.T.D.: Conceptualisation; Methodology; Validation; Investigation; Formal analysis; Data curation; Software; Writing - original draft, T.N.D.; Investigation; Resources; Software; Visualisation; Writing - review & editing, V.D.L.; Conceptualisation; Writing - review & editing; Funding acquisition; Project administration; Supervision. All authors have read and agreed to the published version of the manuscript.

Conflicts of Interest: The authors declare no conflict of interest.

Supplementary material: Can be found at the following link:

https://ijred.cbiore.id/index.php/ijred/article/downloadSuppFile/61561/15931

Data availability: Data will be made available on request.

References

Abagnale, C., Cardone, M., Iodice, P., Strano, S., Terzo, M., & Vorraro, G. (2015). A dynamic model for the performance and

environmental analysis of an innovative e-bike. *Energy Procedia*, 81, 618–627. https://doi.org/10.1016/j.egypro.2015.12.046
Asaei, B., & Habibidoost, M. (2010). A new energy control strategy for a through-the-road parallel hybrid electric motorcycle. 2010 *IEEE Vehicle Power and Propulsion Conference (VPPC)*, 1–5. IEEE. https://doi.org/10.1109/VPPC.2010.5729135
Alagmy, A. R., Mohamed, E. A., Ahmed, A. A., & El-Sherif, M. (2024). Design and development of drivetrain system for electric motorcycles. 2024 *25th International Middle East Power System Conference (MEPCON)*. IEEE. https://doi.org/10.1109/MEPCON63025.2024.10850416
Asaei, B., & Habibidoost, M. (2013). Design, simulation, and prototype production of a through-the-road parallel hybrid electric motorcycle. *Energy Conversion and Management*, 71, 12–20. https://doi.org/10.1016/j.enconman.2013.03.016
Aprillia, B. S., Silalahi, D. K., Raharjo, J., Rokhmat, M., Furkhan, M. F., & Wijaya, F. A. S. (2023). Design of a 72 V 40 Ah electrical system battery pack for electric motorcycle. *In 2023 3rd ICE3IS* (pp. 432–435). IEEE. https://doi.org/10.1109/ICE3IS59323.2023.10335309
Arifwardana, J., Rushadiawan, I., Tjahjana, D., Nizam, M., & Putra, M. (2022). Experimental of heat generation on electric motorcycle NMC and LiFePO4 battery pack. *In 2022 7th ICEVT* (pp. 173–176). IEEE. https://doi.org/10.1109/ICEVT55516.2022.9924981
Arricale, V. M., Brancati, R., Carputo, F., Maiorano, A., & Dell'Annunziata, G. N. (2021). Non-linear motorcycle dynamic model for stability and handling analysis with roll motion and longitudinal speed regulation. *In VEHITS* (pp. 292–300). https://doi.org/10.5220/0010386802920300
Arshad, K., Hussain, N., Ashraf, M. H., & Saleem, M. Z. (2024). Air pollution and climate change as grand challenges to sustainability. *Science of The Total Environment*, 172370. https://doi.org/10.1016/j.scitotenv.2024.172370
Awirya, A. A., Sembiring, D. P., & Kreuta, B. (2023). The potential development of electric motorcycles in remote areas case study: Agats District, Asmat Regency, Indonesia. *Cleaner Engineering and Technology*, 17, 100690. https://doi.org/10.1016/j.clet.2023.100690
Brodsky, P., Fan, G., & Canova, M. (2016). Battery pack design and optimization for the OSU Buckeye current 2016 electric racing motorcycle. *In 2016 ESARS-ITEC Conference* (pp. 1–6). IEEE. https://doi.org/10.1109/ESARS-ITEC.2016.7841436
Buy A123 Products. (2025). Battery specification PDF. Retrieved from https://www.buya123products.com/uploads/vipcase/468623916e3ecc5b8a5f3d20825eb98d.pdf
Chen, H.-C., Li, S.-S., Wu, S.-L., & Lee, C.-Y. (2021). Design of a modular battery management system for electric motorcycle. *Energies*, 14(12), 3532. https://doi.org/10.3390/en14123532
Chen, B.-C., Lin, C.-C., Hwang, J.-J., & Chen, Y.-L. (2004). Modeling and control of hybrid electric motorcycle with direct-driven wheel motor. *SAE Transactions*, 113(6), 785–791. https://www.jstor.org/stable/44723551
Chen, W., Xiao, H., Wang, Q., Zhao, L., & Zhu, M. (2016). Integrated vehicle dynamics and control. *John Wiley & Sons*. https://www.wiley.com/en-us/Integrated+Vehicle+Dynamics+and+Control-p-9781118380024
DNK Power. (2019). Samsung INR21700-50E datasheet. Retrieved from https://www.dnkpower.com/wp-content/uploads/2019/02/SAMSUNG-INR21700-50E-Datasheet.pdf
DNK Power. (2022). LG INR21700 M50LT cell specification. Retrieved from https://www.dnkpower.com/wp-content/uploads/2022/07/LG-INR21700_M50LT_-CELL-SPECIFICATION.pdf
DNK Power. (2025). 5000mAh 21700 battery. Retrieved from https://www.dnkpower.com/5000mah-21700-battery/
Driga, A. M., & Drigas, A. S. (2019). Climate change 101: How everyday activities contribute to the ever-growing issue. *International Journal of Recent Contributions to Engineering, Science & IT*, 7(1), 22–31. https://doi.org/10.3991/ijes.v7i1.10031
Du, W., Zhang, D., & Zhao, X. (2009). Dynamic modelling and simulation of electric bicycle ride comfort. In 2009 *International Conference on Mechatronics and Automation* (pp. 4339–4343). IEEE. https://doi.org/10.1109/ICMA.2009.5246586
Elbeshbeshy, A. M., et al. (2023). Design and development of a low-cost battery system for electric motorcycles. *In 2023 24th MEPCON* (pp. 1–7). IEEE. https://doi.org/10.1109/MEPCON58725.2023.10462347
Esparza, P., Castano-Solis, S., Jiménez-Bermejo, D., Fraile Ardanuy, J., & Merino, M. (2020). Experimental determination of the energetic performance of a racing motorcycle battery-pack. *Processes*, 8(11), 1391. https://doi.org/10.3390/pr8111391
EVLithium. (2025). 32Ah high energy density lithium pouch cell. Retrieved from https://www.evlithium.com/hot-lithium-battery/32ah-high-energy-density-lithium-pouch-cell.html and https://www.swe.com/media/files/files/a8e04d60/kokam-lc-cell-msds_8fusKnZ.pdf
EVLithium. (2025). A123 Battery 506. Retrieved from https://www.evlithium.com/A123-Battery/506.html and https://www.alibaba.com/product-introduction/A123-Nanophosphate-Lithium-Ion-Battery-Prismatic_1600151789405.html
Fahma, F., Sutopo, W., Pujiyanto, E., & Nizam, M. (2024). Dynamic open innovation to determine technology-based interoperability requirement for electric motorcycle swappable battery. *Journal of Open Innovation: Technology, Market, and Complexity*, 10(2), 100259. https://doi.org/10.1016/j.joitmc.2024.100259
Guerra, E. (2019). Electric vehicles, air pollution, and the motorcycle city: A stated preference survey of consumers' willingness to adopt electric motorcycles in Solo, Indonesia. *Transportation Research Part D: Transport and Environment*, 68, 52–64. https://doi.org/10.1016/j.trd.2017.07.027
Hanifah, R. A., Toha, S. F., Hanif, N. H. H. M., & Kamisan, N. A. (2019). Electric motorcycle modeling for speed tracking and range travelled estimation. *IEEE Access*, 7, 26821–26829. https://doi.org/10.1109/ACCESS.2019.2900443
Hima, S., Nehaoua, L., Seguy, N., & Arioui, H. (2007). Motorcycle dynamic model synthesis for two-wheeled driving simulator. *In 2007 IEEE Intelligent Transportation Systems Conference* (pp. 812–817). IEEE. https://doi.org/10.1109/ITSC.2007.4357729
Huang, S. K., Kuo, L., & Chou, K.-L. (2018). The impacts of government policies on green utilization diffusion and social benefits–A case study of electric motorcycles in Taiwan. *Energy Policy*, 119, 473–486. https://doi.org/10.1016/j.enpol.2018.04.061
Izzaturrahman, A., Athallah, R. A. N., & Raharjo, J. (2025). Design of 64 V 24 Ah battery pack with Li-ion 1865 cells for two-wheels electric vehicle. *In Journal of Physics: Conference Series* (Vol. 2942, No. 1, p. 012010). IOP Publishing. https://doi.org/10.1088/1742-6596/2942/1/012010
Kusumah, S., Zahran, R., & Raharjo, J. (2025). Design of a LiFePO4 battery pack 21 A for electric motorcycle. *In Journal of Physics: Conference Series* (Vol. 2942, No. 1, p. 012020). IOP Publishing. https://doi.org/10.1088/1742-6596/2942/1/012020
LeBel, F.-A., Pelletier, L., Messier, P., & Trovao, J. P. (2018). Battery pack sizing method-case study of an electric motorcycle. *In 2018 IEEE Vehicle Power and Propulsion Conference* (VPPC) (pp. 1–6). IEEE. https://doi.org/10.1109/VPPC.2018.8604955
Li, S., Khan, Z., Tan, D., Liu, G., & Zahid, H. (2023). Role of renewable energy and fiscal policy on trade-adjusted carbon emissions: Evaluating the role of environmental policy stringency. *Renewable Energy*, 205, 156–165. https://doi.org/10.1016/j.renene.2023.01.047
Li, Y. (2025). A study on rigid-flexible coupling virtual prototype modeling for motorcycle dynamics. *Third International Conference on Advanced Materials and Equipment Manufacturing* (AMEM 2024), 13691. SPIE. https://doi.org/10.1117/12.3069504
Makarchuk, D., et al. (2015). Analysis of energies and speed profiles of driving cycles for fuel consumption measurements. *In 14th International Scientific Conference on Engineering for Rural Development* (Jelgava) (pp. 265–271).
MathWorks. Mixed-Integer Linear Programming Algorithms, "intlinprog," MathWorks Help Center. Accessed: Feb. 18, 2024. [Online]. Available: https://www.mathworks.com/help/optim/ug/intlinprog.html
Moreno Giner, D., & Manka, M. (2009). Motorcycle dynamic models for virtual rider design and cornering analysis. *In International Design Engineering Technical Conferences and Computers and Information in*

Engineering Conference (Vol. 49033, pp. 869–878). https://doi.org/10.1115/DETC2009-86823

Morandin, M., Ferrari, M., & Bolognani, S. (2014). Power-train design and performance of a hybrid motorcycle prototype. *IEEE Transactions on Industry Applications*, 51(3), 2216–2226. https://doi.org/10.1109/TIA.2014.2360955

Murtiningrum, A. D., Darmawan, A., & Wong, H. (2022). The adoption of electric motorcycles: A survey of public perception in Indonesia. *Journal of Cleaner Production*, 379, 134737. https://doi.org/10.1016/j.jclepro.2022.134737

Niccolai, A., Bonfitto, A., Martelli, M., & Marzoli, M. (2025). Two-wheel-driven electric superbike powertrain optimization. arXiv preprint arXiv:2503.23984. https://doi.org/10.48550/arXiv.2503.23984

Niccolai, A., Bonfitto, A., Martelli, M., & Marzoli, M. (2024). Analysis of energy consumption for electric motorcycles depending on vehicle configuration and driving cycles. *IOP Conference Series: Materials Science and Engineering*, 1306(1), 012021. IOP Publishing. https://doi.org/10.1088/1757-899X/1306/1/012032

Nugraha, M. R., & Kartini, E. (2022). The analysis of Li-ion battery pack 48V 15Ah performance for electric bike. *In AIP Conference Proceedings*, 2708(1). AIP Publishing. https://doi.org/10.1063/5.0123489

Nguyen, V.-T., Hwang, P., & Huynh, T. (2017). Computational analysis on hybrid electric motorcycle with front wheel electric motor using lithium-ion battery. *2017 International Conference on System Science and Engineering (ICSSE)*, 131–135. IEEE. https://doi.org/10.1109/ICSSE.2017.8030896

Nguyen, V.-T., Anh, P. T., & Thinh, H. (2018). A simulation study on energy consumption and cost analysis of hybrid electric motorcycle. *International Journal of Mechanical Engineering and Applications*, 6(4-1), 1–11. https://doi.org/10.11648/j.ijmea.s.2018060401.11

Nguyen, V. T., Nguyen, T. D., & Pham, A. T. (2020). A study on optimizing the characteristics of lithium-ion battery power source and operating cost for hybrid motorcycle. *VNUHCM Journal of Engineering and Technology*, 3(SI2), SI81–SI92. https://doi.org/10.32508/stdjet.v3iSI2.600

Qu, Z.-W., Cao, N.-B., Chen, Y.-H., Zhao, L.-Y., Bai, Q.-W., & Luo, R.-Q. (2017). Modeling electric bike–car mixed flow via social force model. *Advances in Mechanical Engineering*, 9(9), 1687814017719641. https://doi.org/10.1177/1687814017719641

Salman, M., Chaturvedi, S., & Su, W. (2025). Comprehensive study of e-bike braking dynamics: Modeling, simulation and experimental validation. *IEEE Access*. https://doi.org/10.1109/ACCESS.2025.3532296

Shahjalal, M., et al. (2022). A numerical thermal analysis of a battery pack in an electric motorbike application. *Designs*, 6(4), 60. https://doi.org/10.3390/designs6040060

Sharp, R., Evangelou, S., & Limebeer, D. J. (2004). Advances in the modelling of motorcycle dynamics. *Multibody System Dynamics*, 12, 251–283. https://doi.org/10.1023/B:MUBO.0000049195.60868.a2

Syahrobi, S., Dalimunthe, M. E., & Tharo, Z. (2025). Analysis of lithium-ion battery characteristics in electric motors. *INFOKUM*, 13(2), 445–451. https://doi.org/10.58471/infokum.v13i02.2799

Thejasree, G., & Maniyeri, R. (2019). E-bike system modeling and simulation. *In 2019 IEEE International Conference on Intelligent Systems and Green Technology (ICISGT)* (pp. 9–95). IEEE. https://doi.org/10.1109/ICISGT44072.2019.00017

VinFast. (2025). VinFast Evo 200. Retrieved from https://banggiavinfast.vn/san-pham/vinfast-evo-200/

Willis, M. J., & von Stosch, M. (2017). L0-constrained regression using mixed integer linear programming. *Chemometrics and Intelligent Laboratory Systems*, 165, 29–37. https://doi.org/10.1016/j.chemolab.2016.12.016

Wenzl, H. (2009). Capacity. In J. Garche (Ed.), *Encyclopedia of Electrochemical Power Sources* (pp. 395–400). Elsevier. https://doi.org/10.1016/B978-044452745-5.00043-5

Yuniarto, M. N., Wiratno, S. E., Nugraha, Y. U., Sidharta, I., & Nasruddin, A. (2022). Modeling, simulation, and validation of an electric scooter energy consumption model: A case study of Indonesian electric scooter. *IEEE Access*, 10, 48510–48522. https://doi.org/10.1109/ACCESS.2022.3171860

Zahedi, R., Pourezzat, A. A., & Jafari, M. (2024). Hybrid energy storage system for electric motorcycles: Technical and economic analysis. *Case Studies in Thermal Engineering*, 60, 104613. https://doi.org/10.1016/j.csite.2024.104613

Zaripov, R., & Gavrilovs, P. (2019). Study of dynamic characteristics of electric bicycles. *Procedia Computer Science*, 149, 307–313. https://doi.org/10.1016/j.procs.2019.01.140

Zhu, S., Nishimura, H., Iwamatsu, S., & Tajima, H. (2008). Dynamical analysis of motorcycle by multibody dynamics approach. *Journal of System Design and Dynamics*, 2(3), 703–714. https://doi.org/10.1299/jsdd.2.703